

ELECTRONIC SUPPORTING INFORMATION

Tadpole-like cationic single-chain nanoparticles display high cellular uptake

Yen Vo¹, Radhika Raveendran¹, Cheng Cao¹, Linqing Tian¹, Rebecca Y. Lai¹, Martina H. Stenzel^{1}*

¹School of Chemistry, University of New South Wales, Sydney, New South Wales 2052, Australia

Contents

List of Figures	2
List of Tables.....	4
List of Schemes.....	4
Analytical instruments	5
Size Exclusion Chromatography.....	5
Nuclear Magnetic Resonance Spectroscopy (NMR)	5
UV-Visible Spectroscopy (UV-Vis)	5
Fluorescence Spectroscopy.....	5
Dynamic Light Scattering (DLS).....	5
Transmission Electron Microscope (TEM).....	6
Small angle X-ray scattering (SAXS).....	6
Synthesis	7
Synthesis of RAFT agent	7
Synthesis of polymer backbones.....	10
Polymer backbones with different charge types	10
Polymer backbones with increased charge density.....	11
Polymer backbones with different charge positions	12
Synthesis of crosslinker	13
Deprotection of tert-butyl groups.....	15
Results.....	16
Charge type	16
Charge density	34
Charge Position.....	39
Crosslinking density.....	43
References.....	44

List of Figures

Figure S1. ^1H NMR spectrum of RAFT M- CPP in CDCl_3 .	8
Figure S2. ^{13}C NMR spectrum of RAFT M- CPP in CDCl_3 .	9
Figure S3. Illustration of the preparation of polymer backbones with different charge types (a), densities (b), and positions (c) via PET-RAFT polymerization.	10
Figure S4. ^1H NMR spectrum of polymer 15% AET in CDCl_3 .	16
Figure S5. ^1H NMR spectrum of polymer tBA in CDCl_3 .	17
Figure S6. ^1H NMR spectrum of polymer HEA in CDCl_3 .	17
Figure S7. ^1H NMR spectrum of polymer tBA-AET in CDCl_3 .	18
Figure S8. ^1H NMR spectrum of polymer AEA in CDCl_3 .	18
Figure S9. SEC traces of polymer backbones with different charge types. Data was collected from a refractive index (RI) detector. DMF was used as the eluent.	19
Figure S10. ^1H NMR spectrum of 4-(2-(2-methoxy-4-(2-(quinolin-2-yl)vinyl)phenoxy)ethoxy)-4-oxobutanoic acid (QIS) DMSO-d_6 .	20
Figure S11. ^1H NMR spectrum of copolymer P-15% AET in CDCl_3 .	20
Figure S12. ^1H NMR spectrum of copolymer P-tBA in CDCl_3 .	21
Figure S13. ^1H NMR spectrum of copolymer P-HEA in CDCl_3 .	21
Figure S14. ^1H NMR spectrum of copolymer P- tBA-AET in CDCl_3 .	22
Figure S15. ^1H NMR spectrum of copolymer P-AEA in CDCl_3 .	22
Figure S16. SEC traces of polymer with different charge types before (blue) and after (red) crosslinker conjugation. Data was collected from IR detection, and DMF was used as the eluent.	23
Figure S17. SEC traces of polymers with different charge types (a), densities(b,) and positions (c) in aqueous solvent. Data was collected from an RI detector, with 40 vol% acetonitrile and 0.1 vol% TFA in water as the eluent.	24
Figure S18. SAXS plots of polymer with different charge types (a), densities (b), and positions (c) in water. Polymer concentration at 5 mg mL^{-1} .	25
Figure S19: Volume-weighted hydrodynamic size distribution of polymer samples with different charge types (a), densities (b), and positions (c) in water. Polymer concentration at 1 mg mL^{-1} in water.	25
Figure S20. The light chamber set-up for the crosslinking step. The chamber consists of 144 blue LED lights ($\lambda_{\text{max}} \approx 453 \text{ nm}$).	26
Figure S21. UV-Vis spectra of P-15% AET sample after irradiation under blue light at different times. The polymer solution is at 1 mg mL^{-1} in water, and the arrow shows the reduction of the quinoline peak after a specific irradiation time.	26
Figure S22. ^1H NMR spectra of the copolymer in CDCl_3 before (P-tBA, upper) and after (P-AA, lower) deprotection of tert-butyl groups.	30
Figure S23. ^1H NMR spectra of copolymer in CDCl_3 before (P-tBA-AET, upper) and after (S-AA-AET, lower) deprotection of tert-butyl groups.	31

Figure S24. CLSM images of MCF-7 cells incubated with SCNPs with different charge types. Cells were incubated with Cy5-labeled NPs (red) at a concentration of 100 $\mu\text{g mL}^{-1}$, 4°C for 2 hours. Nuclei and membrane were stained with Hoechst (blue) and wheat germ agglutinin (WGA) (green), respectively. This figure has the same setting as Figure 2c .	32
Figure S25. Stability study of SCNPs with different charge types at 37°C in complete DMEM cell medium. Data was collected from DLS over time, and the polymer concentration was 1 mg mL^{-1} .	33
Figure S26. ^1H NMR spectrum of copolymer 10% AET in CDCl_3 .	34
Figure S27. ^1H NMR spectrum of copolymer 20% AET in CDCl_3 .	34
Figure S28. ^1H NMR spectrum of copolymer 30% AET in CDCl_3 .	35
Figure S29. SEC traces in DMF of polymer backbones with different charge densities. Data was collected from RI detection, and DMF was used as the eluent.	35
Figure S30. ^1H NMR spectrum of copolymer P-10% AET in CDCl_3 .	36
Figure S31. ^1H NMR spectrum of copolymer P-20% AET in CDCl_3 .	36
Figure S32. ^1H NMR spectrum of copolymer P-30% AET in CDCl_3 .	37
Figure S33. SEC traces of polymer with different charge densities before (blue) and after (red) crosslinker conjugation. Data was collected from RI detection, and DMF was used as the eluent.	37
Figure S34. Stability study of SCNPs with different charge densities at 37°C in complete DMEM cell medium. Data was collected from DLS over time; polymer concentration is 1 mg mL^{-1} .	38
Figure S35. ^1H NMR spectrum of copolymer RD AET in CDCl_3 .	39
Figure S36. ^1H NMR spectrum of copolymer Mid AET in CDCl_3 .	39
Figure S37. ^1H NMR spectrum of copolymer HnT AET in DMSO-d_6 .	40
Figure S38. SEC traces of polymer backbones with different charge positions. Data was collected from RI detection, and DMF was used as the eluent.	40
Figure S39. ^1H NMR spectrum of copolymer P-Mid AET in CDCl_3 .	41
Figure S40. ^1H NMR spectrum of copolymer P-RD AET in CDCl_3 .	41
Figure S41. ^1H NMR spectrum of copolymer P-HnT AET in CDCl_3 .	42
Figure S42. SEC traces of polymers with different charge positions before (blue) and after (red) the crosslinker conjugation. Data was collected from RI detection, and DMF was used as the eluent.	42
Figure S43. Stability study of SCNPs with different charge positions at 37°C in complete DMEM cell medium. Data was collected from DLS over time. Polymer concentration is 1 mg mL^{-1} .	43
Figure S44. Stability study of SCNPs with different crosslinking densities at 37°C in complete DMEM cell medium. Data was collected from DLS over time, and the polymer concentration was 1 mg mL^{-1} .	43

List of Tables

Table S1. Reaction condition and monomer conversion of each step for the synthesis of polymers with different charge densities.	12
Table S2. Polymerization conditions for the preparation of the second block of copolymer with different charge types.	16
Table S3. Molecular weight analysis of the polymer-crosslinker conjugates.	24
Table S4. Optimized crosslinking conditions for the polymers with different charge types. Polymer solution in water at a concentration of 1 mg mL ⁻¹	27
Table S5. Characterization of polymer nanoparticles before and after crosslinking	28
Table S6. Hydrodynamic size and polydispersity index (PDI) of polymer samples before and after crosslinking, collected from DLS number and volume distributions. Polymer samples were measured at a concentration of 1 mg mL ⁻¹ in water.	29

List of Schemes

Scheme S1. Procedure for the synthesis of RAFT agent M-CPP.	7
Scheme S2. Procedure for the synthesis of crosslinker QIS	14

Analytical instruments

Size Exclusion Chromatography

Size exclusion chromatography (SEC) in DMF was performed using a Shimadzu Prominence modular SEC system coupled with an LC-20AD pump, a RID-20A detector, a SIL-20A HT autosampler, and a guard column. Three Phenomenex columns (pore sizes of 10^3 , 10^4 , and 10^5 Å) were used for separation while *N,N*-dimethylformamide (DMF) (HPLC grade) containing 0.05 % w/v BHT, 0.01 % w/v LiBr was used as the eluent. The system was operated at a flow rate of 0.8 mL min^{-1} with the isocratic solvent mode at 50°C in a CTO-20A oven. The injection volume was $50 \mu\text{L}$. The unit was calibrated using polymethyl methacrylate (PMMA) commercial standards.

SEC traces in water were collected from an Agilent HPLC 1260 Infinity System, equipped with a quaternary pump. The column used for separation was Superdex 200 Increase 5/150 GL (cytiva). MilliQ water was used as the eluent at a flow rate of 0.45 mL min^{-1} .

Nuclear Magnetic Resonance Spectroscopy (NMR)

Nuclear Magnetic Resonance (NMR) Spectroscopy was utilized for the structural characterization of the synthesized compounds and for determining the conversion of the polymerization reaction. Both ^1H NMR and ^{13}C NMR spectra were acquired using an autosampler system integrated into a Bruker Advance III 400 MHz spectrometer. The NMR spectra were processed and analyzed using MestReNova software. For NMR measurements, CDCl_3 , DMSO-d_6 , and D_2O were employed as the measuring solvents, depending on the specific requirements of the samples.

UV-Visible Spectroscopy (UV-Vis)

UV-Visible Spectroscopy (UV-Vis) was utilized to monitor the conversion of the dimerization reaction during the crosslinking process. The data were recorded using a VARIAN Bio UV-Visible Cary 60 UV-Vis Spectrophotometer equipped with a Perkin Elmer Differential Scanning Calorimeter, with an absorbance range of less than 5 Abs and a wavelength range of 200-800 nm. Measurements were conducted over the visible range ($\lambda = 400\text{-}800 \text{ nm}$) at a temperature of 25°C .

Fluorescence Spectroscopy

The Fluorescence Spectra of Cy5-labeled NPs in water were measured using an Agilent Cary Eclipse fluorescence spectrophotometer. All fluorescence spectra were recorded between 650 and 750 nm with an excitation wavelength (λ_{ex}) of 640 nm and an emission wavelength (λ_{em}) of 660 nm. The entrance and exit slit width were set to 10 mm.

Dynamic Light Scattering (DLS)

DLS measurements were conducted using a Malvern Zetasizer Nano ZS equipped with a He-Ne laser (633 nm, max 5 mW) and a light scattering angle of 173° . The data analysis was performed using Malvern Zetasizer Software version 6.20. Before measurement, all samples were prepared in Milli-Q water at various concentrations and filtered through a $0.45 \mu\text{m}$ pore size filter to remove dust.

Transmission Electron Microscope (TEM)

The TEM micrographs were captured using a JEOL1400 transmission electron microscope equipped with a dispersive X-ray analyzer and a Gatan CCD camera for digital image acquisition. The measurements were performed at an accelerating voltage of 80 kV. Sample preparation involved casting the micellar solution onto a copper grid, followed by air drying and negative staining with uranyl acetate. TEM size distribution analysis was conducted using Image J, with 100 particles analyzed for each sample.

Small angle X-ray scattering (SAXS)

Small-angle X-ray scattering (SAXS) measurements were conducted at the Australian Synchrotron's SAXS/WAXS beamline¹ using a 96-well plate autoloading system for injecting particle solutions into a capillary. Isotropic scattering patterns were captured with a Pilatus 1 M detector (Dectris, Baden-Daettwil, Switzerland) employing a wavelength of 1.033 Å (12 KeV) and a sample-to-detector distance of 2.3 m. The measurement geometry facilitated the conversion of counts per detector pixel to radially averaged intensity of the scattering vector on an absolute scale. Background scattering from the solvent in the capillary was subtracted using the beamline software Scatterbrain.

SAXS curves were acquired under 5 mg/mL particle solution, emphasizing the particle shape and size (form factor). Data analysis involved parameter optimization for structural models based on measured data. Poly Gauss Coil model was applied in SAXS data analysis. Fitting parameters were optimized using SASview² or specific macros developed for IgorPro.³

Diffusion-Ordered NMR Spectroscopy (DOSY-NMR)

Diffusion-Ordered NMR Spectroscopy (DOSY-NMR) was used to determine the diffusion coefficients of linear polymers and their corresponding SCNPs. DOSY NMR measurements were conducted manually using a Bruker Advance III 400 MHz. All measurements were carried out in D₂O at 5°C. The radius of particles was calculated *via* the Stoke-Einstein equation.

$$R_H = (k_B \times T) / 6\pi\eta D \quad (\text{Equation 1})$$

Where:

k_B : the Boltzmann constant

T: temperature (K)

η : liquid's viscosity

D: the diffusion coefficient measured by DOSY NMR

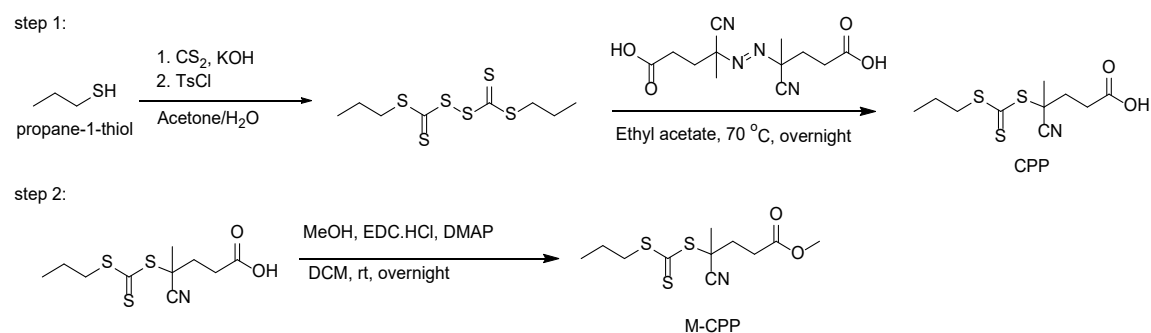
Fitted function:	$e^{-D \times \gamma^2 \times g^2 \times \delta^2 (\Delta - \delta/3 - \tau/2)} \times 10^4$
used gamma:	26752 rad/(s*Gauss)
used little delta:	0.0070000 s
used big delta:	0.074900 s
used gradient strength:	variable

Random error estimation of data:	RMS per spectrum (or trace/plane)
Systematic error estimation of data:	worst case per peak scenario
Fit parameter Error estimation method:	from fit using arbitrary y uncertainties
Confidence level:	95%
Used integrals:	area integral
Used Gradient strength:	all values (including replicates) used

Synthesis

Synthesis of RAFT agent

The RAFT agent was prepared as shown in **Scheme S1**.⁴



Scheme S1. Procedure for the synthesis of RAFT agent M-CPP

Step 1: Synthesis of 4-cyano-4-(((propylthio)carbonothioyl)thio)pentanoic acid (CPP)

The synthesis of the RAFT agent CPP involved several steps with modifications.⁴ In a 200 mL glass round bottom flask, an aqueous solution of KOH (2.24g, 2 eq.) was slowly added dropwise to a prepared solution of propane-1-thiol (20 mmol, 1.53 g, 1 eq.) in acetone (50 mL). The mixture was stirred for 10 minutes before adding carbon disulfide (1.51 mL, 1.25 eq.), followed by stirring for an additional 2 hours. Subsequently, a prepared solution of 4-toluenesulfonyl chloride (4.57 g, 1.2 eq.) in acetone (20 mL) was slowly added dropwise to the flask, and the mixture was stirred overnight.

After the reaction was completed, the organic solvent was removed using a rotary evaporator, and the crude product was extracted with ethyl acetate and washed several times with water (3 × 100 mL). The intermediate product was then purified by column chromatography on silica gel using a hexane-ethyl acetate mixture (5 vol % ethyl acetate in hexane) as the eluent. The isolated yield of the red liquid intermediate product was 84%.

In the subsequent step, the purified intermediate product (2.6474 g, 1.25 eq.) and 4,4'-azobis(4-cyanovaleric acid) (VA501, containing 18% water, w/w) (2.3926 g, 1 eq.) were dissolved in ethyl acetate (100 mL). The solution was subjected to three freeze-pump-thaw cycles to degas it before being placed in an oil bath at 70°C under a nitrogen atmosphere overnight. After the reaction, the

organic solvent was removed using a rotary evaporator, and the crude product was purified by column chromatography on silica gel using a hexane-ethyl acetate mixture (1:3 v/v) as the eluent. The isolated yield of the yellow solid product was 67%.

Step 2: Preparation of methyl 4-cyano-4-(((propylthio)carbonothioyl)thio) pentanoate (M-CPP)

The condensation reaction between the carboxylic group on the CPP RAFT agent and methanol was employed. In a 25 mL round bottom flask, CPP (1.43g, 5.2 mmol) and 4-dimethylaminopyridine (DMAP) (0.31 g, 0.5 eq.) were dissolved in 10 mL of dichloromethane (DCM). The CPP solution was then slowly added dropwise to a prepared solution containing methanol (10.4 mL, 50 eq.) and 1-ethyl-3-(3-dimethylaminopropyl)carbodiimide hydrochloride (EDC·HCl) (1.98 g, 2 eq.). The reaction mixture was allowed to react at room temperature overnight. After completion of the reaction, the solvent was removed using a rotary evaporator, and the crude product was purified by column chromatography on silica gel using a hexane-ethyl acetate mixture (2:1 v/v) as the eluent. The isolated yield of the yellow liquid product was 90%.

^1H NMR (400 MHz, CDCl_3) δ 3.73 (s, 3H), 3.39 – 3.30 (m, 2H), 2.69 – 2.50 (m, 3H), 2.40 (ddd, $J = 14.1, 9.3, 6.7$ Hz, 1H), 1.90 (s, 3H), 1.76 (h, $J = 7.3$ Hz, 2H), 1.05 (t, $J = 7.4$ Hz, 3H).

^{13}C NMR (101 MHz, CDCl_3) δ 216.96, 171.90, 118.98, 52.10, 46.36, 38.84, 33.88, 29.59, 24.85, 21.29, 13.47.

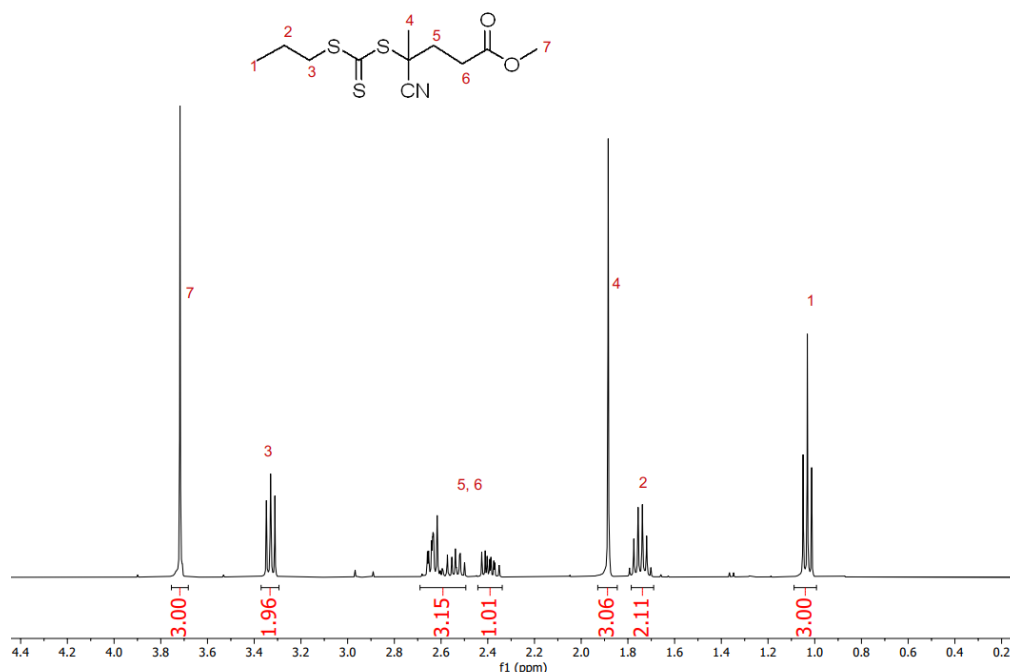


Figure S1. ^1H NMR spectrum of RAFT M- CPP in CDCl_3 .

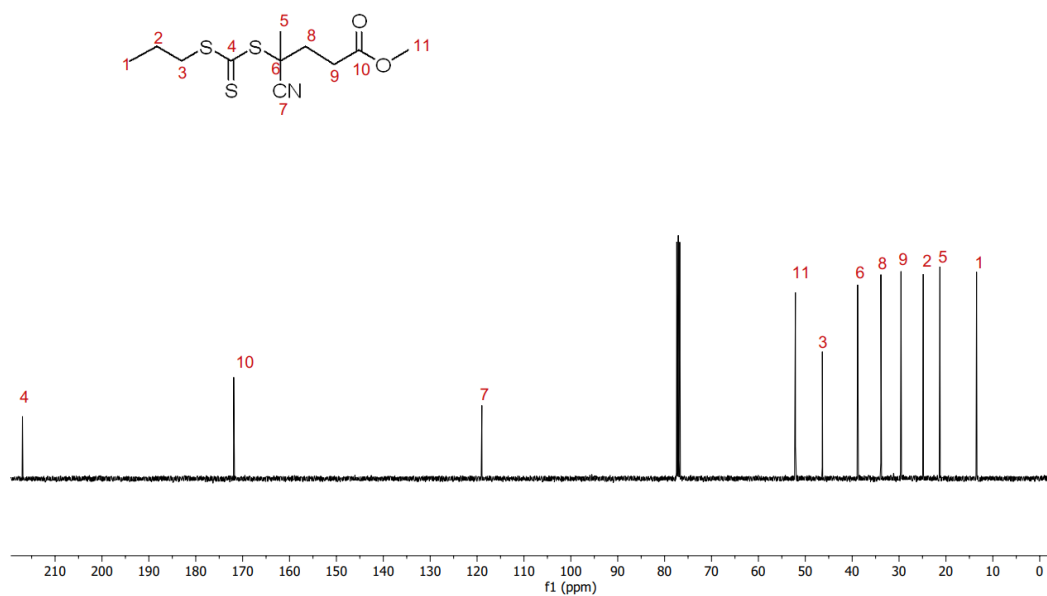


Figure S2. ^{13}C NMR spectrum of RAFT M- CPP in CDCl_3 .

Synthesis of polymer backbones

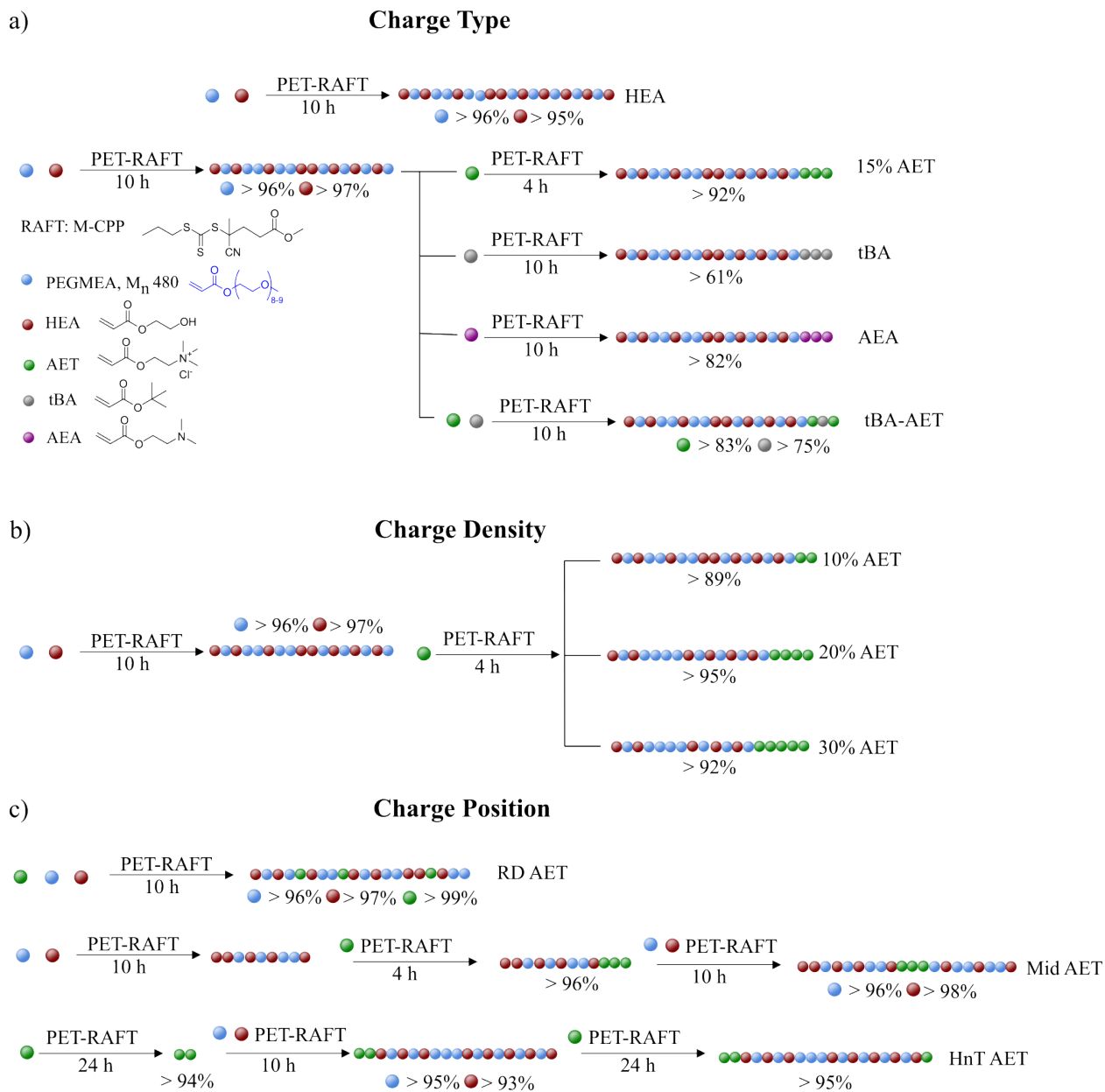


Figure S3. Illustration of the preparation of polymer backbones with different charge types (a), densities (b), and positions (c) *via* PET-RAFT polymerization.

Polymer backbones with different charge types

For the preparation of non-charged polymer, namely HEA, the polymerization of PEGMEA and HEA *via* PET-RAFT was employed (Error! Reference source not found.2). The solution of poly(ethylene glycol) methyl ether acrylate (PEGMEA) (2.4 g, 5 mmol), 2-hydroxyethyl acrylate (HEA) (0.42 g, 3.6 mmol), and M-CPP (0.02 g, 0.069 mmol) in 1.5 mL DMSO was prepared.

Next, 250 μL of mesitylene (as an external standard) and 700 μL of 0.002 M Zn TPP solution were added, and the solution was stirred for 5 minutes before being irradiated for 10 hours under LED yellow light ($\lambda = 565 \text{ nm}$, 2 mW cm^{-2}). The feed ratio of PEGMEA: HEA: M-CPP: Zn TPP was 72:52:1:0.02. Monomer conversion achieved for PEGMEA was $> 96\%$, and for HEA was $> 95\%$.

For the synthesis of the first statistical block copolymer of P(PEGMEA₇₀-stat-HEA₃₃), PEGMEA, $M_n = 480 \text{ g mol}^{-1}$, (6.26 g, 13 mmol), HEA (0.71 g, 6 mmol), and M-CPP (0.0523 g, 0.18 mmol) were dissolved in 4 mL DMSO in a 20 mL glass vial. Then, 700 μL of mesitylene and 1.8 mL of 0.002 M Zn TPP solution were added to the solution, stirring for 5 min. The ratio of PEGMEA:HEA:M-CPP: Zn TPP was 73:34:1:0.02. Subsequently, 1 mL of the solution was added into thirteen 2 mL glass vials and irradiated for 10 hours under yellow light ($\lambda = 565 \text{ nm}$). Monomer conversion for PEGMEA was $> 96\%$, and for HEA $> 97\%$.

For the synthesis of the second block of charged monomer and/or tert-butyl acrylate (tBA), the solution of the desired monomer in DMSO was prepared and added to a glass vial containing the prepared statistical copolymer of PEGMEA and HEA. The solution in the glass vials was then mixed by vortex for 10 seconds before being irradiated for a specific time under yellow light ($\lambda_{\text{max}} = 565 \text{ nm}$). The feed ratio of the second block monomer and RAFT agent and the irradiation time and conversion for each monomer are summarized in Error! Reference source not found. **S1**.

Polymer backbones with increased charge density

The first statistical block of PEGMEA and HEA and the second charged block were prepared according to the abovementioned procedure. The feed ratio of monomers: RAFT: Zn TPP, irradiation time, and conversion for each step were presented in Error! Reference source not found.. Different charge densities were achieved by adjusting the feed ratio of AET:RAFT. The total DP of all polymers was kept constant, with lines 1 and 5 corresponding to the polymer, namely 10% AET, lines 2 and 6 to 15% AET, lines 3 and 7 to 20% AET, and lines 4 and 8 to 30% AET.

Table S1. Reaction condition and monomer conversion of each step for the synthesis of polymers with different charge densities.

1st Block				
No.	PEGMEA:HEA:RAFT:Zn TPPP	Irradiation time (h)	Conversion	Polymer's name
1	73:39:1:0.02	10	PEGMEA > 96% HEA > 97%	10% AET
2	73:34:1:0.02	10	PEGMEA > 96% HEA > 97%	15% AET
3	73:27:1:0.02	10	PEGMEA > 96% HEA > 97%	20% AET
4	73:16:1:0.02	10	PEGMEA > 96% HEA > 97%	30% AET
2nd Block				
No.	AET:RAFT ratio	Irradiation time (h)	Conversion of AET	Polymer's name
5	13:1	4	> 89%	10% AET
6	22:1	4	> 92%	15% AET
7	26:1	4	> 95%	20% AET
8	39:1	4	> 92%	30% AET

Polymer backbones with different charge positions

For the preparation of RD AET, PEGMEA (2.9 g, 6 mmol), HEA (0.33 g, 2.85 mmol), AET (0.38 g, 1.57 mmol), and M-CPP (0.024 g, 0.082 mmol) were dissolved in 1.54 mL DMSO. Next, 300 μ L of mesitylene and 833 μ L of 0.002 M Zn TPP solution in DMSO were added. The solution was stirred for 5 minutes before being irradiated for 10 hours under yellow light ($\lambda = 565$ nm). The feed ratio of PEGMEA:HEA:AET:M-CPP:Zn TPP was 73:34:19:1:0.02. Monomer conversions achieved were > 96% for PEGMEA, > 97% for HEA, and > 97% for AET.

For the preparation of Mid AET copolymer, the first block of the statistical copolymer of PEGMEA and HEA was prepared *via* PET-RAFT polymerization. PEGMEA (1.93 g, 4 mmol), HEA (0.262 g, 2.26 mmol) and M-CPP (0.0322 g, 0.11 mmol) were dissolved in 1 mL DMSO. Next, 200 μ L of mesitylene and 1.1 mL of 0.002 M Zn TPP solution in DMSO were added. The solution was stirred for 5 min, then 0.5 mL of solution was added to 2 mL glass vials before irradiated for 10 hours under yellow light ($\lambda = 565$ nm). The feed ratio of PEGMEA: HEA: AET:

M-CPP: Zn TPP was 36:20:19:1:0.02. Monomer conversions achieved for PEGMEA was > 96%, and for HEA was > 95%.

For the second block of AET, the solution of AET (0.5 g, 2 mmol) in 1.15 mL DMSO was prepared, and then 200 μ L of the monomer solution was added to each vial containing the first block. Next, the solution in glass vials was mixed by vortex for 10 seconds before being irradiated for 4 hours under yellow light ($\lambda = 565$ nm). The feed ratio of AET:RAFT was 19:1. The conversion achieved was > 96%.

For the third block of PEGMEA and HEA, PEGMEA (1.93 g, 4 mmol) and HEA (0.21 g, 1.8 mmol) were dissolved in 2 mL DMSO. Next, 500 μ L of the monomer solution was added to each vial containing the two prepared blocks and mixed well by vortex for 10 s. The solution was irradiated for 10 hours under yellow light ($\lambda = 565$ nm). The feed ratio of PEGMEA: HEA: RAFT was 36:17:1. Conversion achieved for PEGMEA was > 96%, and for HEA was > 98%.

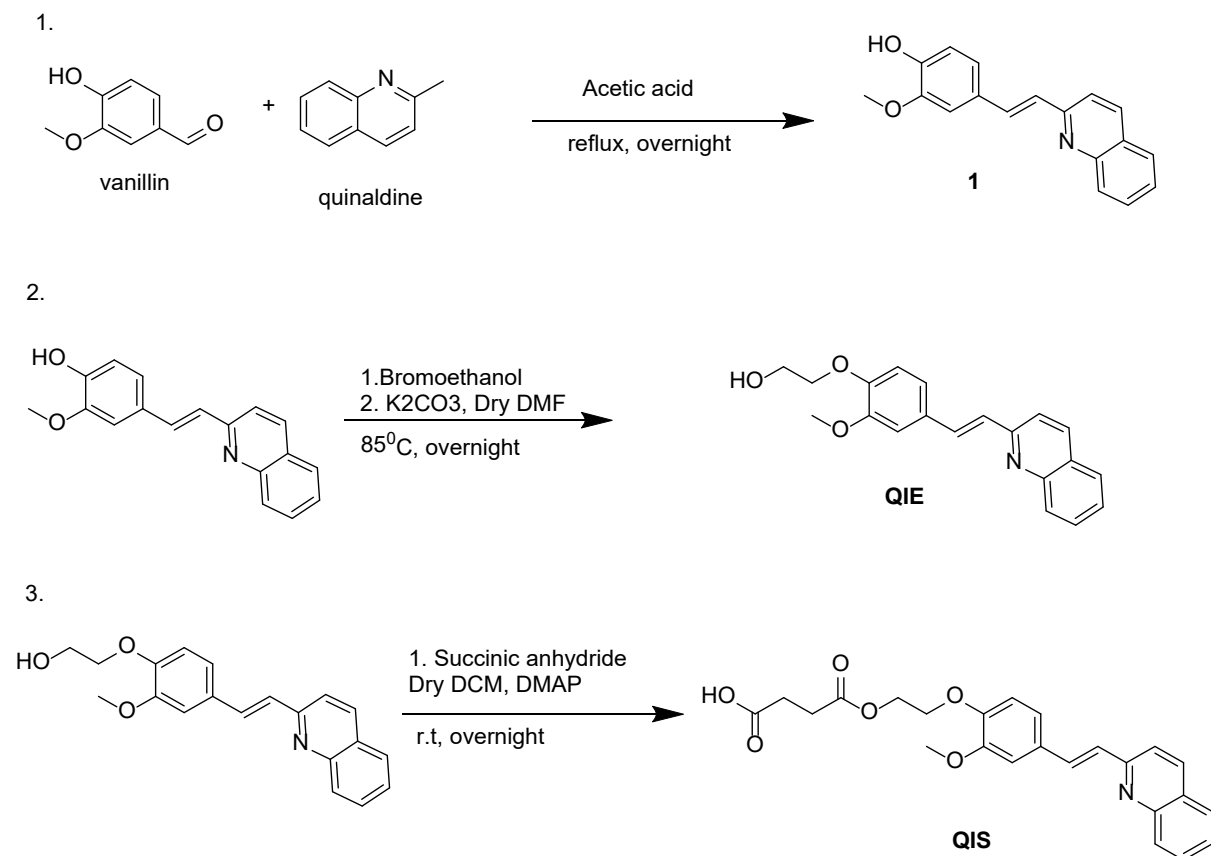
For the preparation of the Mid AET copolymer, the first block of the statistical copolymer of PEGMEA and HEA was prepared *via* PET-RAFT polymerization. PEGMEA (1.93 g, 4 mmol), HEA (0.262 g, 2.26 mmol), and M-CPP (0.0322 g, 0.11 mmol) were dissolved in 1 mL DMSO. Next, 200 μ L of mesitylene and 1.1 mL of 0.002 M Zn TPP solution in DMSO were added. The solution was stirred for 5 min, then 0.5 mL of the solution was added to 2 mL glass vials before being irradiated for 10 hours under yellow light ($\lambda = 565$ nm). The feed ratio of PEGMEA: HEA: AET: M-CPP: Zn TPP was 36:20:19:1:0.02. Monomer conversions achieved for PEGMEA were > 96%, and for HEA, it was > 95%.

For the second block of AET, a solution of AET (0.5 g, 2 mmol) in 1.15 mL DMSO was prepared, and then 200 μ L of the monomer solution was added to each vial containing the first block. Next, the solutions in the glass vials were mixed by vortex for 10 seconds before being irradiated for 4 hours under yellow light ($\lambda = 565$ nm). The feed ratio of AET: RAFT was 19:1. The conversion achieved was > 96%.

For the third block of PEGMEA and HEA, PEGMEA (1.93 g, 4 mmol) and HEA (0.21 g, 1.8 mmol) were dissolved in 2 mL DMSO. Next, 500 μ L of the monomer solution was added to each vial containing the two prepared blocks and mixed well by vortex for 10 s. The solution was irradiated for 10 hours under yellow light ($\lambda = 565$ nm). The feed ratio of PEGMEA: HEA: RAFT was 36:17:1. Conversions achieved for PEGMEA was > 96%, and for HEA, it was > 98%.

Synthesis of crosslinker

The crosslinker 4-(2-(2-methoxy-4-(2-(quinolin-2-yl)vinyl)phenoxy)ethoxy)-4-oxobutanoic acid (QIS) was prepared in a three-step synthesis.



Scheme S2. Procedure for the synthesis of crosslinker QIS

First step: preparation of 2-methoxy-4-(2-(quinolin-2-yl)vinyl)phenol (1)

In a 25 mL round bottom flask, a mixture of quinaldine (2.7 mL, 20 mmol) and vanillin (4.57 g, 1.5 eq.) in 5 mL of acetic acid was prepared. The reaction solution was stirred for 10 minutes before being refluxed at 130°C overnight. The crude solution was collected and extracted by adding 100 mL of DCM and subsequently washed several times with brine (2×100 mL) and saturated NaHCO₃ solution (3×100 mL). The organic solvent was removed by a rotary evaporator, and the crude was purified by column chromatography on silica gel using DCM-ethyl acetate as the eluent (9:1 v/v). A yellow solid with an isolated yield of 57% was obtained.

¹H NMR (400 MHz, CDCl₃) δ 8.09 (dd, *J* = 17.2, 8.3 Hz, 2H), 7.78 (dd, *J* = 8.1, 1.4 Hz, 1H), 7.73 – 7.65 (m, 2H), 7.59 (d, *J* = 16.3 Hz, 1H), 7.49 (ddd, *J* = 8.1, 6.9, 1.2 Hz, 1H), 7.32 – 7.20 (m, 3H), 7.12 (dd, *J* = 8.2, 1.9 Hz, 1H), 6.94 (d, *J* = 8.2 Hz, 1H), 5.99 (s, 1H), 3.95 (s, 3H).

Second step: synthesis of 2-(2-methoxy-4-(2-(quinolin-2-yl)vinyl)phenoxy)ethan-1-ol (QIE)

In the second step, a solution of compound (1) (4.65 g, 16.75 mmol) and K₂CO₃ (4.6 g, 2 eq.) in 50 mL of dry DMF was prepared and stirred for 10 minutes at room temperature. Next, bromoethanol (1.76 mL, 2 eq.) was added dropwise to the prepared solution. The flask was filled with nitrogen before being placed in a hot oil bath at 85°C and reacted overnight. The crude product was extracted with 50 mL of ethyl acetate and subsequently washed several times with 0.5 M HCl (2×30 mL) and brine (3×100 mL). The organic solvent was removed by a rotary evaporator, and

the crude product was purified by column chromatography on silica gel using DCM-ethyl acetate (2:1 v/v) and 0.5% MeOH as the eluent. A yellow solid with an isolated yield of 88% was obtained.

^1H NMR (400 MHz, DMSO) δ 8.32 (d, J = 8.6 Hz, 1H), 8.01 – 7.90 (m, 2H), 7.84 (d, J = 8.6 Hz, 1H), 7.80 – 7.69 (m, 2H), 7.54 (ddd, J = 8.1, 6.9, 1.2 Hz, 1H), 7.43 – 7.35 (m, 2H), 7.23 (dd, J = 8.4, 2.0 Hz, 1H), 7.01 (d, J = 8.4 Hz, 1H), 4.87 (t, J = 5.4 Hz, 1H), 4.02 (t, J = 5.1 Hz, 2H), 3.87 (s, 3H), 3.74 (q, J = 5.2 Hz, 2H).

Third step: synthesis of 4-(2-(2-methoxy-4-(2-(quinolin-2-yl)vinyl)phenoxy)ethoxy)-4-oxobutanoic acid (QIS)

In the final step, a 100 mL solution of QIE (4.64 g, 14.4 mmol), succinic anhydride (2.89 g, 2 eq.), and DMAP (0.88 g, 0.5 eq.) in DCM was prepared. The flask was filled with nitrogen and stirred at room temperature overnight. After the reaction was complete, the organic solvent was removed, and the solid was collected, washed several times with brine, and dried under a vacuum. The isolated yield of the yellow solid was 90%.

^1H NMR (400 MHz, DMSO) δ 8.33 (d, J = 8.6 Hz, 1H), 8.01 – 7.91 (m, 2H), 7.84 (d, J = 8.7 Hz, 1H), 7.82 – 7.71 (m, 2H), 7.54 (ddd, J = 8.1, 6.8, 1.2 Hz, 1H), 7.46 – 7.37 (m, 2H), 7.24 (dd, J = 8.4, 1.9 Hz, 1H), 7.03 (d, J = 8.3 Hz, 1H), 4.37 (dd, J = 5.8, 3.2 Hz, 2H), 4.22 (dd, J = 5.6, 3.5 Hz, 2H), 3.88 (s, 3H), 2.61 – 2.46 (m, 5H).

Deprotection of tert-butyl groups

After the conjugation of the crosslinker and/or Cy5 dye, the polymers containing tBA units (P-tBA and S-tBA AET) were deprotected using trifluoroacetic acid (TFA) to remove the tert-butyl groups and release the carboxylic groups. In a 30 mL glass vial, P-tBA (1 g) was dissolved in 1 mL DCM, then 5 mL of TFA was added dropwise. The solution was stirred overnight at room temperature. After that, the solvent and TFA were removed by stirring with an open cap for a day. Next, 5 mL of MeOH was added, and the solution was collected and dialyzed against MeOH for 3 days. The solvent was removed by a rotary evaporator, and the obtained polymer, after deprotection, was dried under a vacuum. ^1H NMR in CDCl_3 was used to confirm the successful deprotection by the disappearance of the tert-butyl peak at 1.43 ppm.

Results

Charge type

Table S2. Polymerization conditions for the preparation of the second block of copolymer with different charge types.

No.	Monomer	Monomer:RAFT ratio	Irradiation time (h)	Conversion	Polymer's name
1	AET	20:1	4	> 92%	15% AET
2	tBA	28:1	10	> 61%	tBA
3	AEA	22:1	10	> 82%	AEA
4	tBA and AET	(tBA:AET:RAFT) 10:13:1	10	tBA > 75%, AET > 83%	tBA-AET

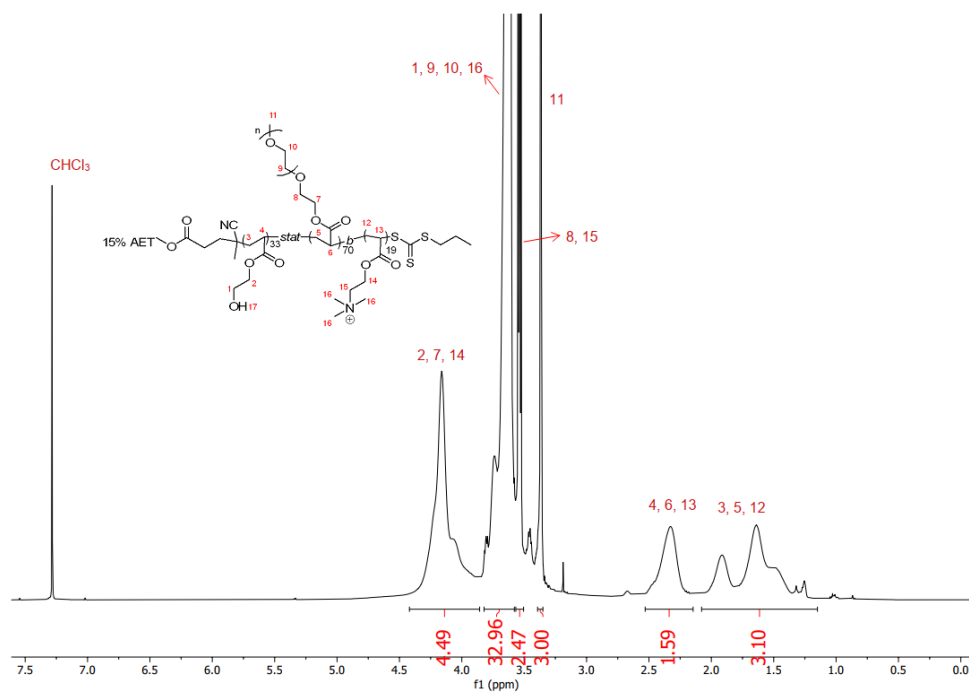


Figure S4. ^1H NMR spectrum of polymer 15% AET in CDCl_3

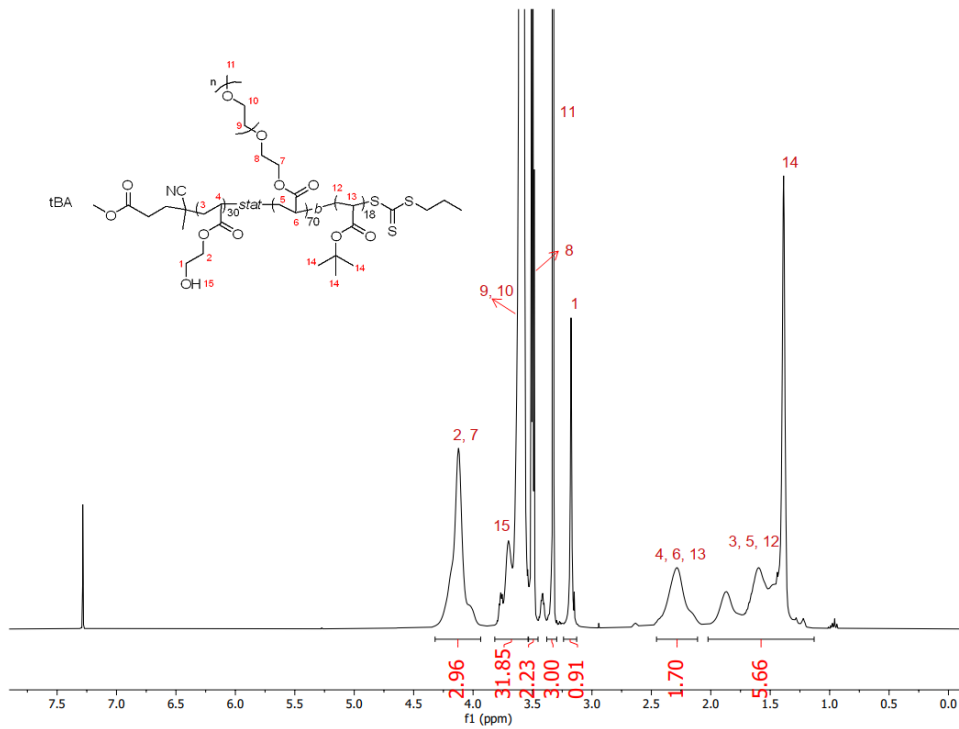


Figure S5. ^1H NMR spectrum of polymer tBA in CDCl_3

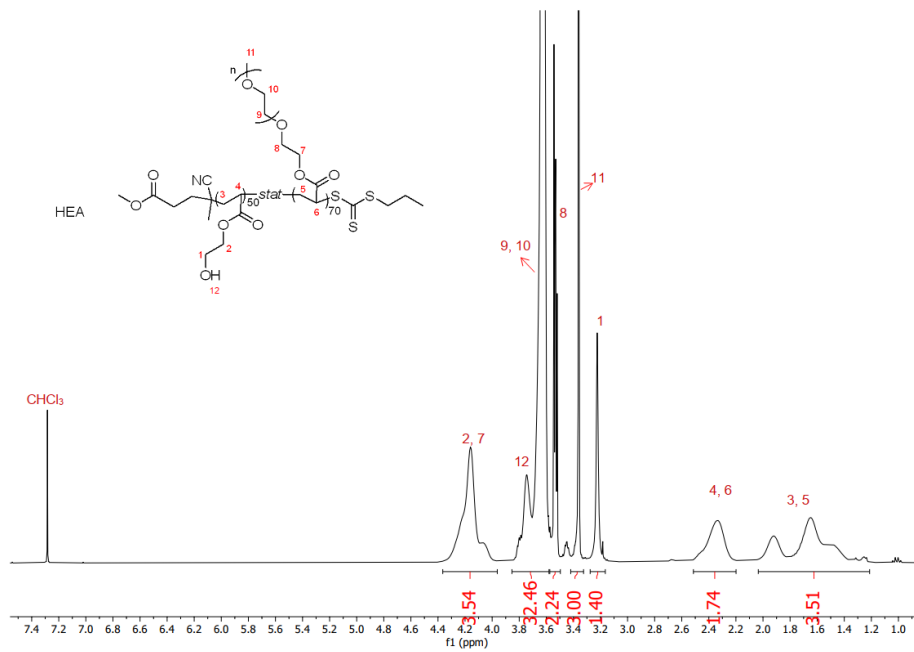


Figure S6. ^1H NMR spectrum of polymer HEA in CDCl_3

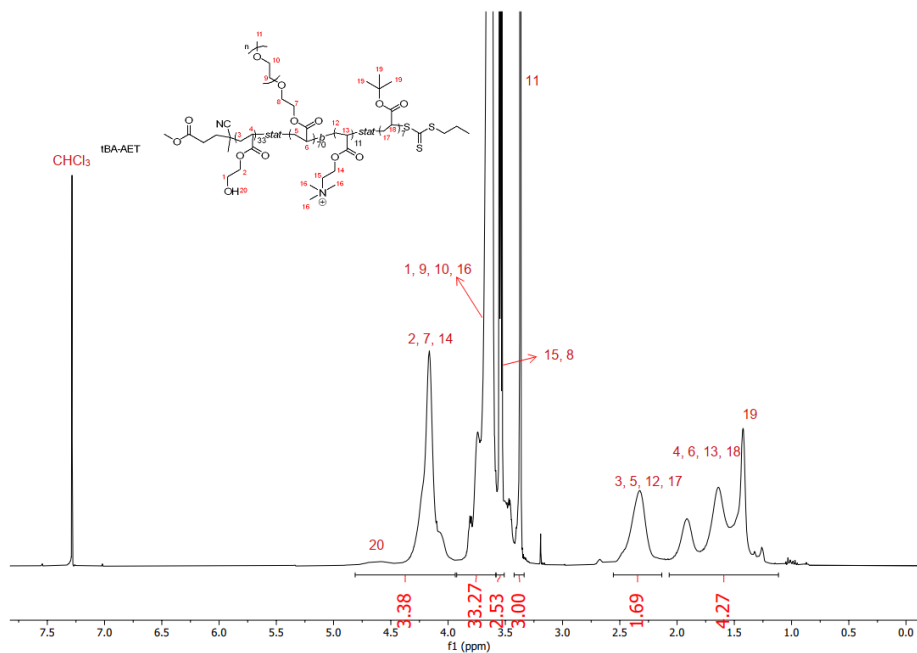


Figure S7. ¹H NMR spectrum of polymer tBA-AET in CDCl₃

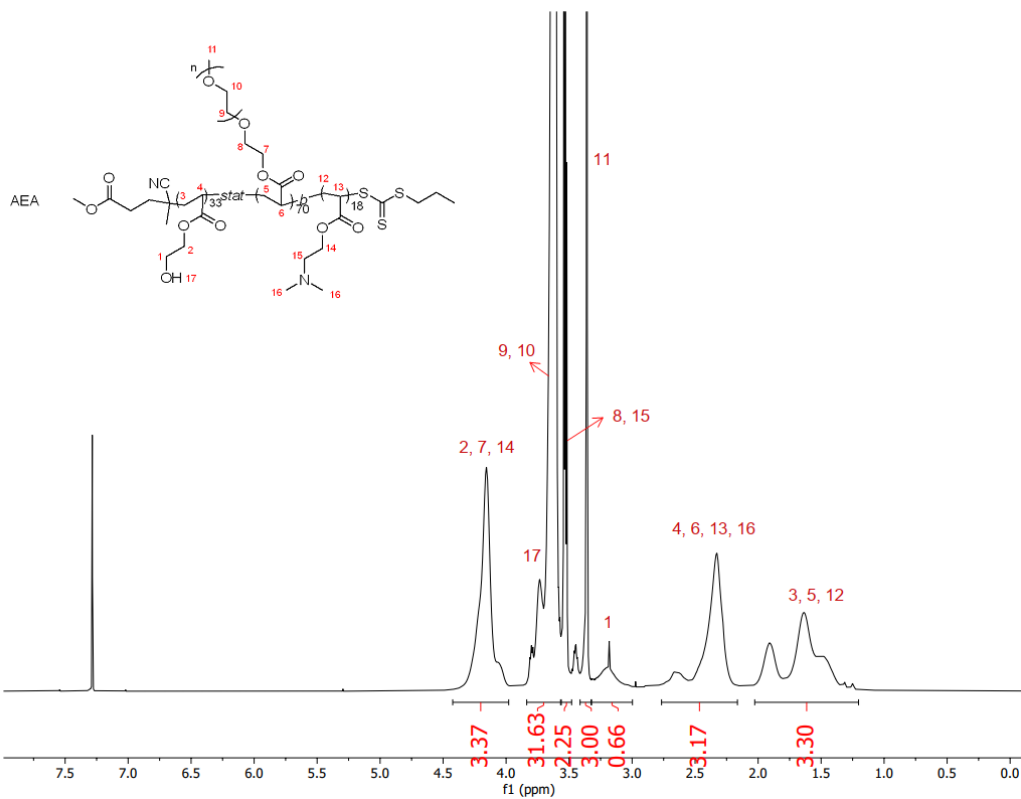


Figure S8. ¹H NMR spectrum of polymer AEA in CDCl₃

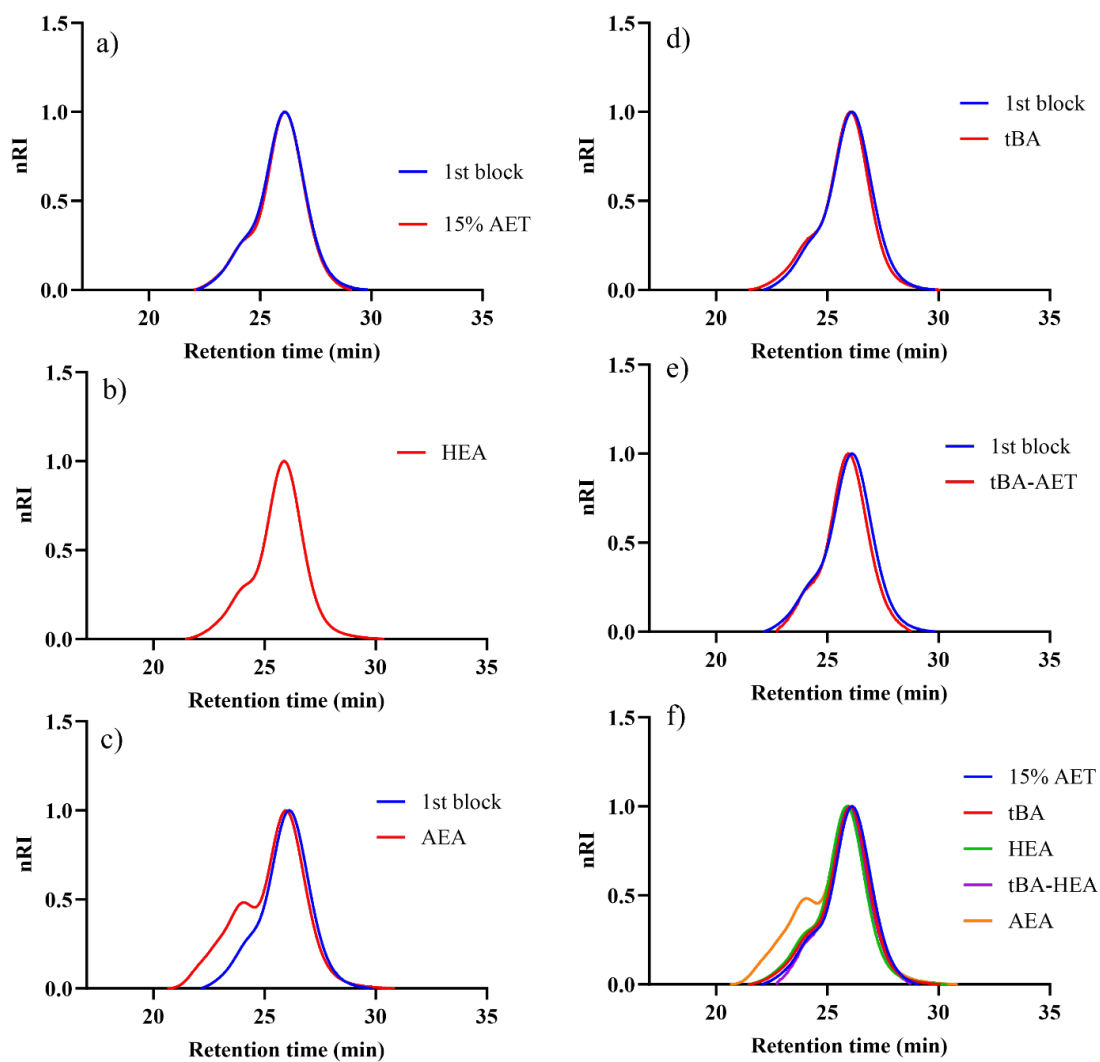


Figure S9. SEC traces of polymer backbones with different charge types. Data was collected from a refractive index (RI) detector. DMF was used as the eluent.

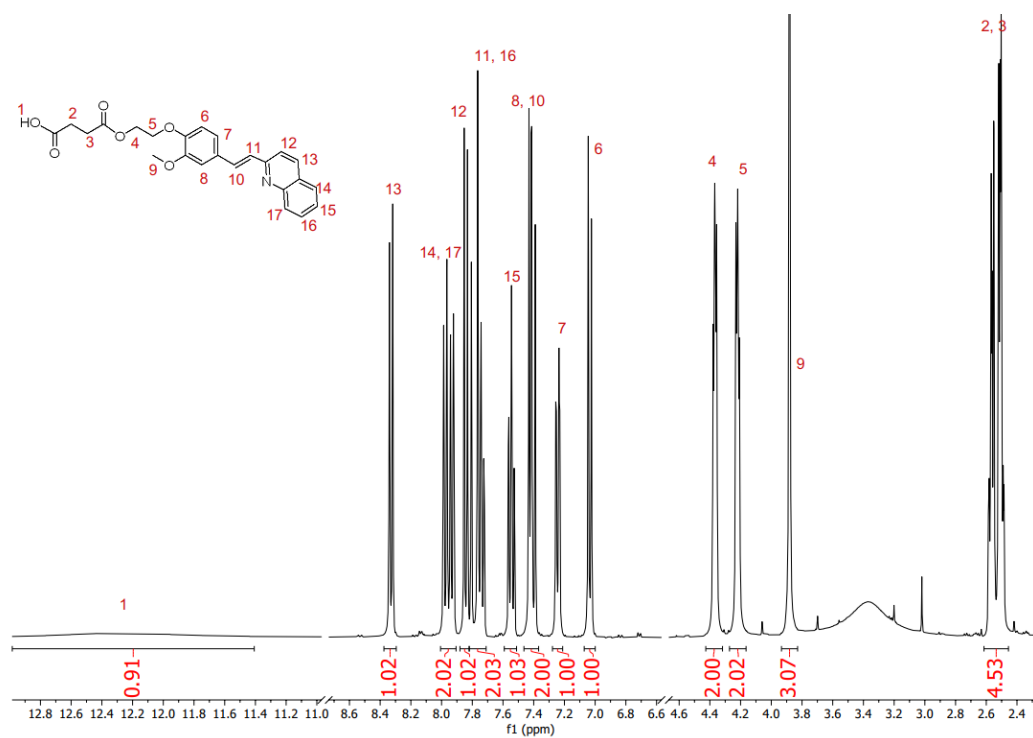


Figure S10. ^1H NMR spectrum of 4-(2-(2-methoxy-4-(2-(quinolin-2-yl)vinyl)phenoxy)ethoxy)-4-oxobutanoic acid (QIS) DMSO- d_6

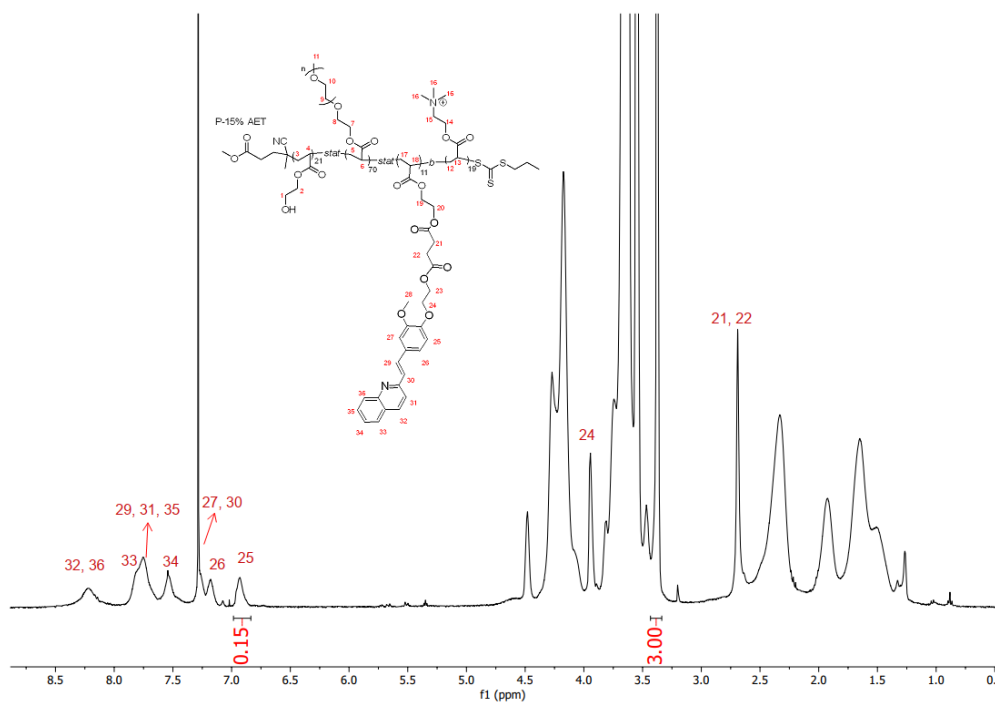


Figure S11. ^1H NMR spectrum of copolymer P-15% AET in CDCl_3 .

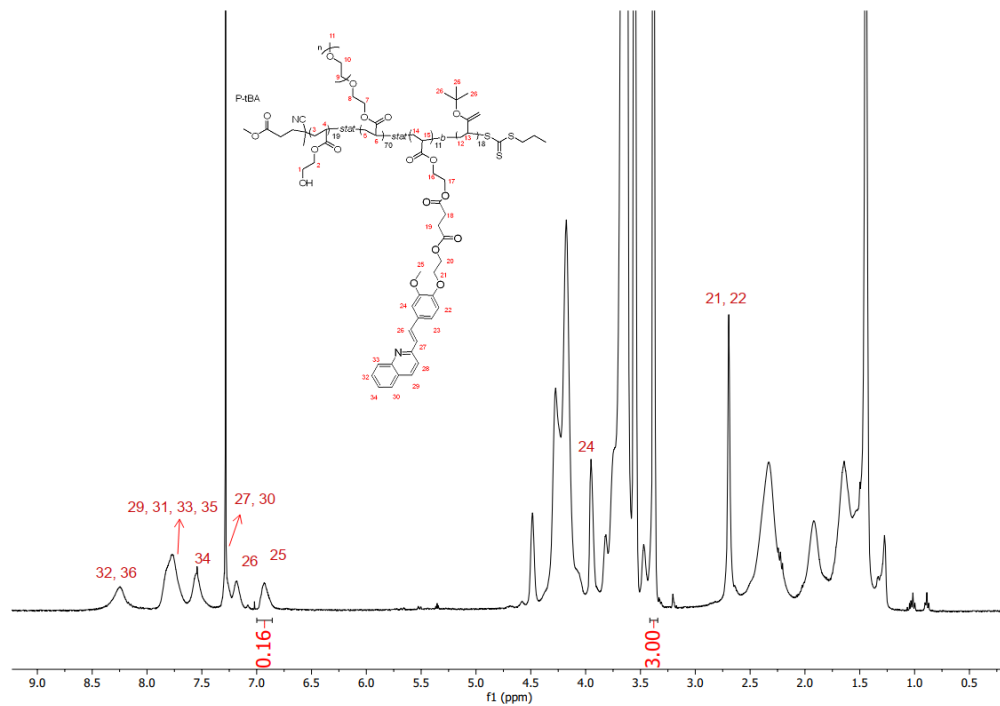


Figure S12. ¹H NMR spectrum of copolymer P-tBA in CDCl₃.

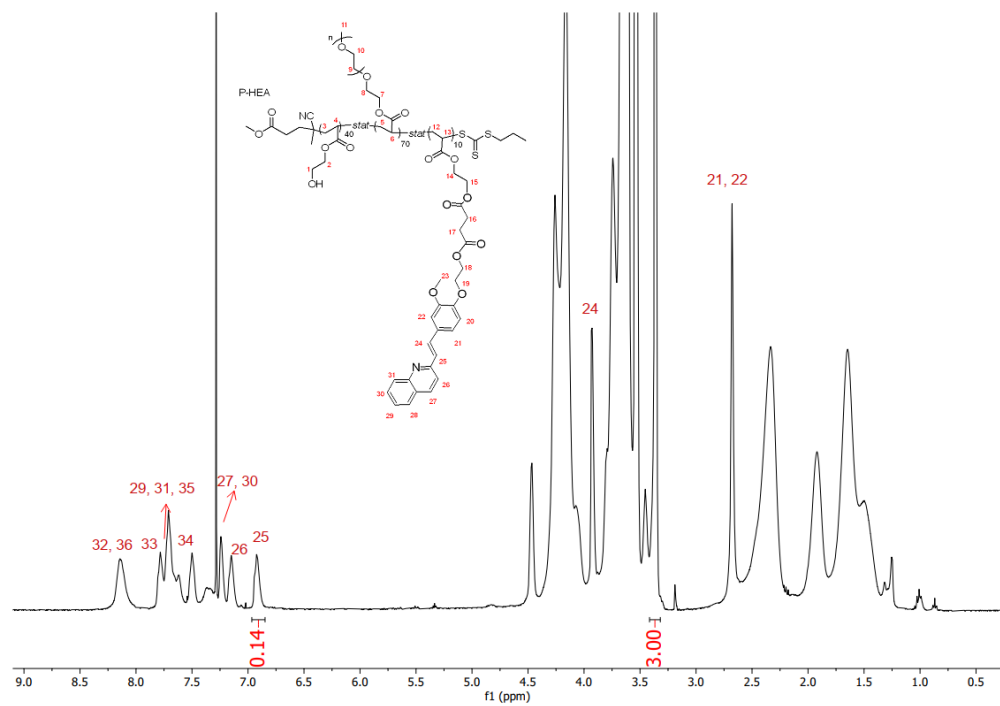


Figure S13. ¹H NMR spectrum of copolymer P-HEA in CDCl₃.

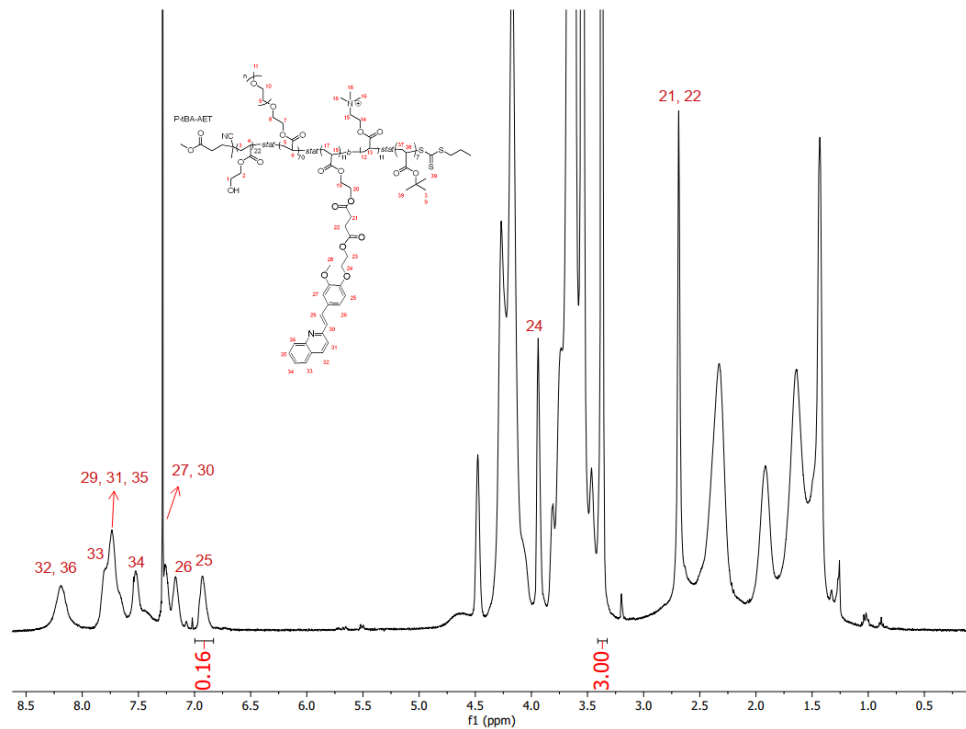


Figure S14. ^1H NMR spectrum of copolymer P-tBA-AET in CDCl_3 .

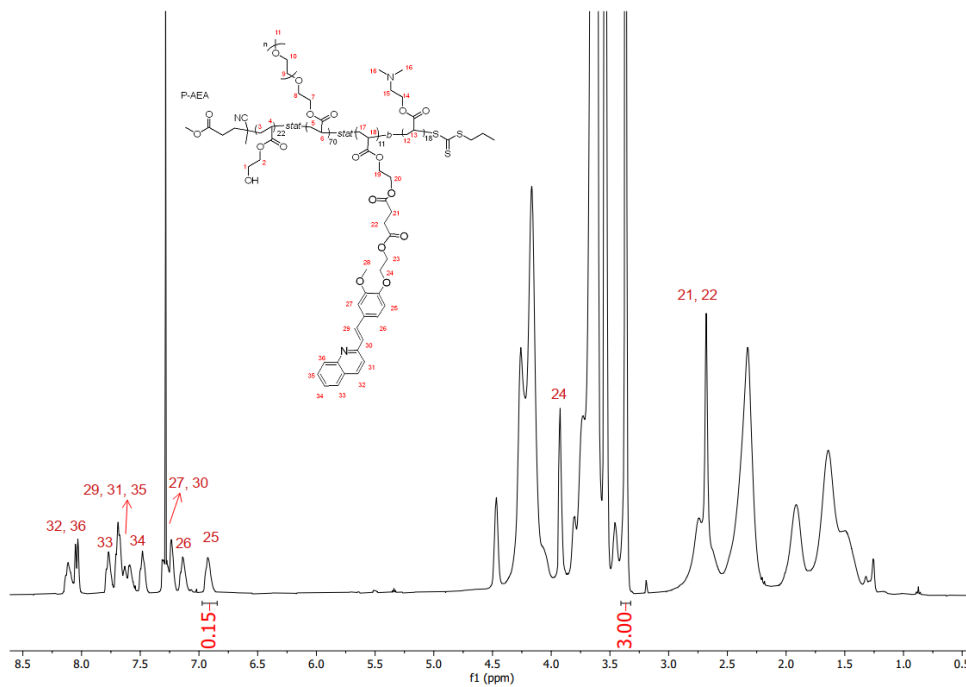


Figure S15. ^1H NMR spectrum of copolymer P-AEA in CDCl_3 .

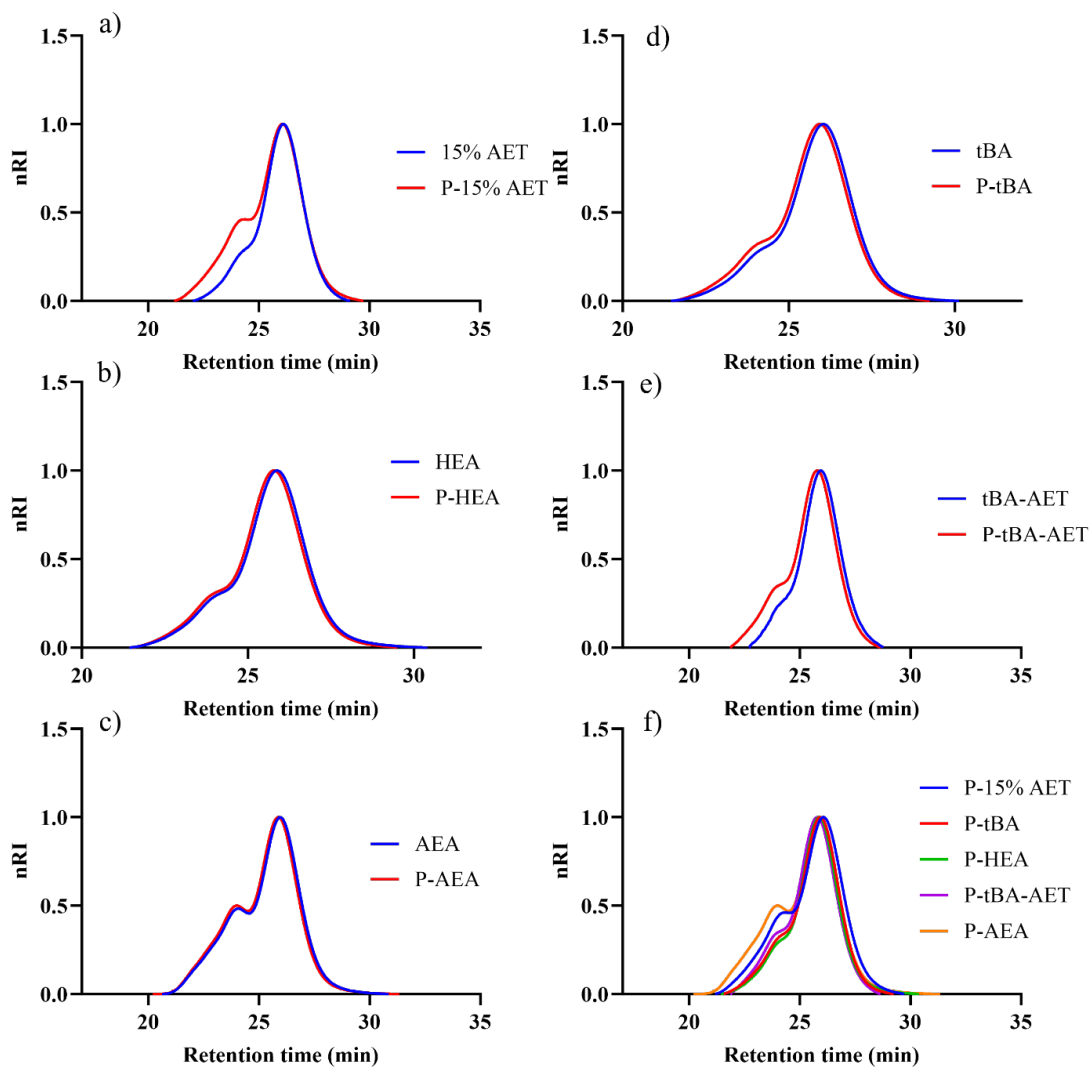


Figure S16. SEC traces of polymer with different charge types before (blue) and after (red) crosslinker conjugation. Data was collected from IR detection, and DMF was used as the eluent.

Table S3. Molecular weight analysis of the polymer-crosslinker conjugates

Polymer	Structure	$M_{n, \text{theo}}^1$	M_n^2	D^2
		(g mol ⁻¹)	(g mol ⁻¹)	
P-15% AET	P(PEGMEA ₇₀ -HEA ₂₂ -QIS ₁₁)- <i>b</i> -PAET ₁₉	45500	36000	1.32
P-tBA	P(PEGMEA ₇₀ -HEA ₁₉ -QIS ₁₁)- <i>b</i> -PtBA ₁₉	43800	35700	1.22
P-HEA	P(PEGMEA ₇₀ -HEA ₄₀ -QIS ₁₀)	43400	36700	1.21
P-tBA-AET	P(PEGMEA ₇₀ -HEA ₂₂ -QIS ₁₁)- <i>b</i> - P(AET ₁₁ -tBA ₇)	44900	37300	1.21
P-AEA	P(PEGMEA ₇₀ -HEA ₂₂ -QIS ₁₁)- <i>b</i> -PAEA ₁₈	44400	39400	1.43
P-10% AET	P(PEGMEA ₇₀ -HEA ₂₇ -QIS ₁₁)- <i>b</i> -PAET ₁₂	44800	36000	1.23
P-20% AET	P(PEGMEA ₇₀ -HEA ₁₆ -QIS ₁₀)- <i>b</i> -PAET ₂₅	45500	34100	1.17
P-30% AET	P(PEGMEA ₇₀ -HEA ₅ -QIS ₁₀)- <i>b</i> -PAET ₃₆	46300	3200	1.24
P-Mid AET	P(PEGMEA ₇₁ -HEA ₂₆ -QIS ₁₀)- <i>b</i> -PAET ₁₈	45800	36700	1.28
P-RD AET	P(PEGMEA ₇₁ -HEA ₂₅ -QIS ₉)- <i>b</i> -PAET ₁₉	45300	74000	1.86
P-HnT AET	P(PEGMEA ₆₈ -HEA ₂₂ -QIS ₈)- <i>b</i> -AET ₂₀	43200	44500	1.56

¹: calculated from ¹H NMR

²: obtained from SEC traces in DMF

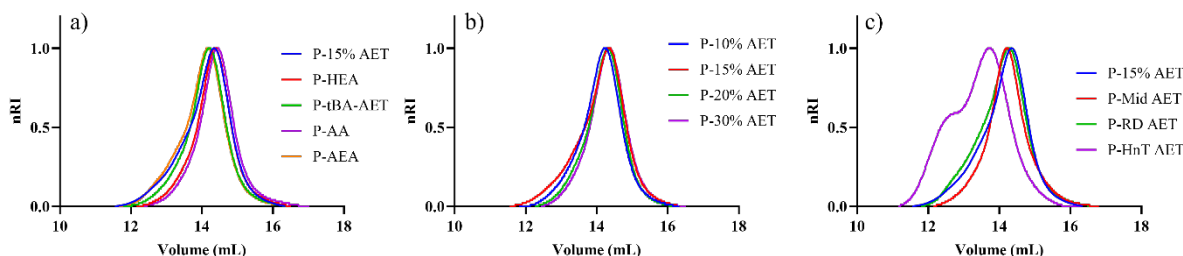


Figure S17. SEC traces of polymers with different charge types (a), densities (b), and positions (c) in aqueous solvent. Data was collected from an RI detector, with 40 vol% acetonitrile and 0.1 vol% TFA in water as the eluent.

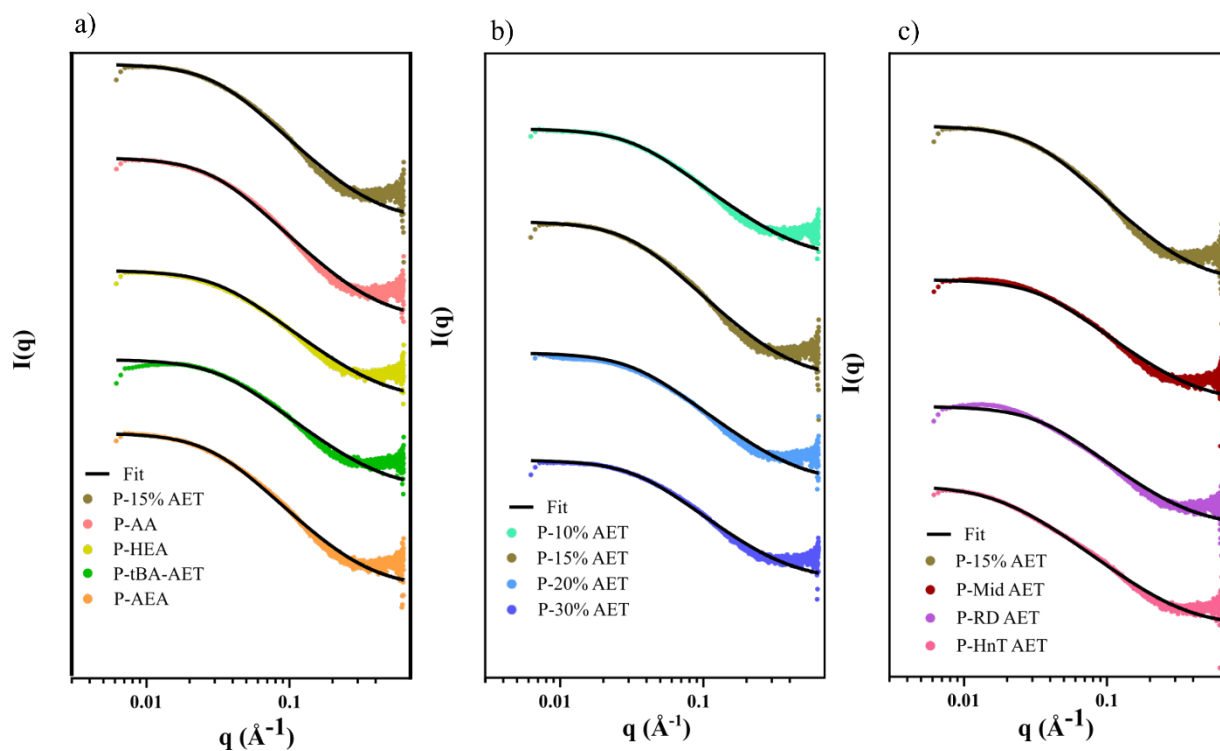


Figure S18. SAXS plots of polymer with different charge types (a), densities (b), and positions (c) in water. Polymer concentration at 5 mg mL^{-1} .

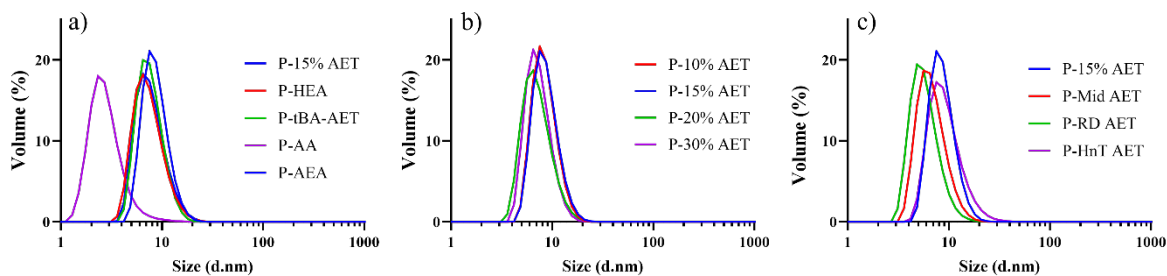


Figure S19: Volume-weighted hydrodynamic size distribution of polymer samples with different charge types (a), densities (b), and positions (c) in water. Polymer concentration at 1 mg mL^{-1} in water.

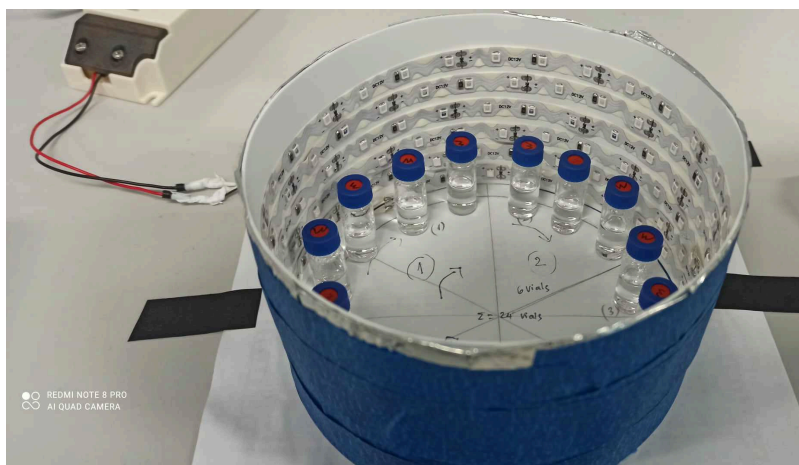


Figure S20. The light chamber set-up for the crosslinking step. The chamber consists of 144 blue LED lights ($\lambda_{\text{max}} \approx 453 \text{ nm}$).

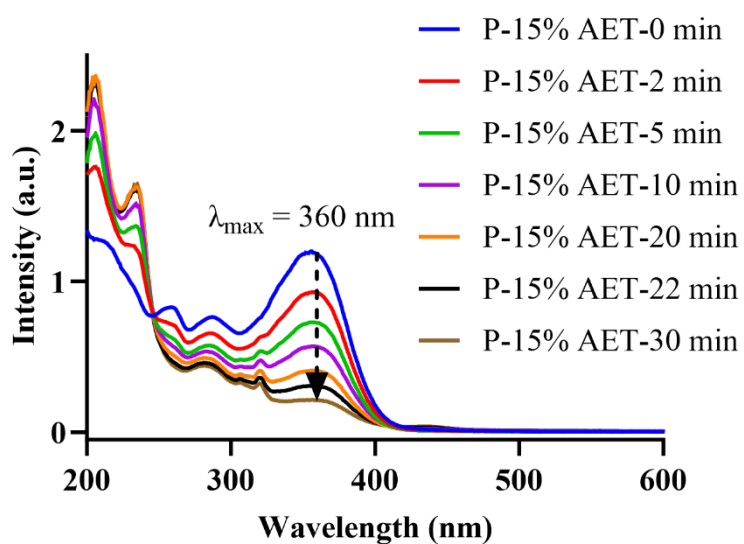


Figure S21. UV-Vis spectra of P-15% AET sample after irradiation under blue light at different times. The polymer solution is at 1 mg mL^{-1} in water, and the arrow shows the reduction of the quinoline peak after a specific irradiation time.

Table S4. Optimized crosslinking conditions for the polymers with different chare types. Polymer solution in water at a concentration of 1 mg mL⁻¹.

	No.	Sample	Irradiation time (min)	Conversion*
Different charges	1	P-15% AET	22	74%
	2	P-AA	5	75%
	3	P-HEA	25	75%
	4	P-tBA-AET	30	73%
	5	P-AEA	30	70%
Charge density	1	P-10% AET	20	73%
	2	P-15% AET	22	74%
	3	P-20% AET	20	77%
	4	P-30% AET	20	74%
Charge position	1	P-15% AET	22	74%
	2	P-Mid AET	25	70%
	3	P-HnT AET	20	70%
	4	P-RD AET	20	75%
Crosslinking density*	1	S-15% AET-1	4	25%
	2	S-15% AET-2	12	53%
	3	S-15% AET-3	26	73%
	4	S-15% AET-4	60	88%

*: At concentration 5 mg ml⁻¹

Table S5. Characterization of polymer nanoparticles before and after crosslinking

	Before crosslinking					After crosslinking						
	Polymer	Diameter (nm)				Polymer	Diameter (nm)				Zeta potential (mV)	R_g/R_h
		DLS ¹	DOSY - NMR ³	SAXS ⁴	R_g/R_h		DLS ¹	DOSY-NMR ³	SAXS ⁴	TEM ²		
Type of charge	P-15% AET	11.2 ± 0.2	9.1	9.6	0.86	S-15% AET	14.2 ± 0.1	9.4	9.6	5.3 ± 1.1	15.1 ± 1.1	0.68
	P-AA	5.1 ± 1.2	8.3	10.2	2.00	S-AA	7.1 ± 0.4	8.1	10.0	13.9 ± 4.4	1.9 ± 0.3	1.41
	P-HEA	11.3 ± 0.5	8.2	9.6	0.85	S-HEA	11.7 ± 0.3	8.4	9.8	11.8 ± 4.7	-14.5 ± 0.8	0.84
	P-tBA-AET	10.0 ± 0.1	8.5	9.2	0.92	(S-tBA-AET)/ S-AA-AET	(10.8 ± 0.1)	(9.5)/ 10.2	(9.2)/16.6	18.6 ± 6.7	(15.8 ± 1.6)/ -3.9 ± 0.1	N.D.
	P-AEA	11.7 ± 0.1	8.5	10.4	0.89	S-AEA	13.9 ± 0.5	8.5	10.6	3.2 ± 0.6	-4.9 ± 1.0	0.76
Charg	P-10% AET	10.7 ± 0.1	9.4	9.6	0.90	S-10% AET	10.8 ± 0.3	9.2	9.6	4.1 ± 0.8	18.3 ± 0.6	0.89
	P-20% AET	10.3 ± 0.3	10.7	9.2	0.89	S-20% AET	9.7 ± 0.2	11.1	9.2	4.4 ± 1.3	26.6 ± 0.5	0.95
	P-30% AET	9.4 ± 0.3	10.3	9.0	0.96	S-30% AET	9.8 ± 0.3	10.6	9.0	6.9 ± 1.7	34.7 ± 0.8	0.92
Charg	P-Mid AET	9.7 ± 0.1	8.7	9.6	0.99	S-Mid AET	9.3 ± 0.1	7.7	9.6	5.6 ± 1.4	19.5 ± 1.9	1.03
	P-HnT AET	18.8 ± 2.0	11.2	14.0	0.74	S-HnT AET	19.8 ± 0.6	12.9	13.8	15.5 ± 8.5	12.2 ± 0.2	0.7
	P-RD AET	8.4 ± 0.4	9.6	10.6	1.26	S-RD AET	10.4 ± 0.7	9.9	10.6	6.0 ± 1.6	6.7 ± 0.7	1.02
Crosslinki	P-15% AET	10.7 ± 0.4	8.46	10.8	1.01	S-15% AET-1	10.9 ± 0.1	8.52	10.8	-	10.5 ± 0.3	0.99
						S-15% AET-2	10.6 ± 0.1	8.75	11.0	-	9.8 ± 0.2	1.04
						S-15% AET-3	10.9 ± 0.7	8.75	11.8	-	9.6 ± 0.3	1.08
						S-15% AET-4	10.4 ± 0.5	8.85	12.0	-	8.9 ± 0.1	1.15

¹: collected from Size peak in DLS Intensity, polymer concentration is 1 mg ml⁻¹ in water.

²: in water

³: calculated from diffusion coefficient, polymer concentration is 8 mg ml⁻¹ in D₂O

⁴: calculated by using Poly Gauss Coil model. Polymer concentration at 5 mg mL⁻¹ in water.

Table S6. Hydrodynamic size and polydispersity index (PDI) of polymer samples before and after crosslinking, collected from DLS number and volume distributions. Polymer samples were measured at a concentration of 1 mg mL⁻¹ in water.

	Samples	Diameter (nm)		PDI
		DLS Number	DLS Volume	
Charge Type	P-15% AET	7.5 ± 0.3	12.0 ± 1.2	0.66 ± 0.02
	S-15% AET	5.9 ± 0.2	8.2 ± 0.2	0.26 ± 0.01
	P-AA	2.3 ± 0.3	3.6 ± 0.3	0.74 ± 0.06
	S-AA	2.8 ± 0.3	4.6 ± 0.3	0.58 ± 0.3
	P-HEA	6.0 ± 0.0	8.2 ± 0.3	0.18 ± 0.02
	S-HEA	5.7 ± 0.1	7.5 ± 0.2	0.16 ± 0.02
	P-tBA-AET	6.5 ± 0.1	8.0 ± 0.1	0.59 ± 0.01
	S-tBA-AET	5.4 ± 0.3	7.3 ± 0.4	0.28 ± 0.03
	P-AEA	6.4 ± 0.1	8.3 ± 0.1	0.3 ± 0.03
	S-AEA	4.9 ± 0.3	8.1 ± 0.4	0.25 ± 0.03
Charge Density	P-10% AET	7.3 ± 0.1	9.4 ± 0.5	0.87 ± 0.02
	S-10% AET	5.7 ± 0.4	7.3 ± 0.3	0.41 ± 0.02
	P-20% AET	5.9 ± 0.1	7.7 ± 0.4	0.61 ± 0.01
	S-20% AET	4.9 ± 0.2	6.4 ± 0.2	0.54 ± 0.01
	P-30% AET	6.3 ± 0.1	8.7 ± 0.3	0.68 ± 0.01
	S-30% AET	4.3 ± 0.1	5.7 ± 0.1	0.57 ± 0.01
Charge Position	P-Mid AET	5.6 ± 0.1	7.0 ± 0.1	0.43 ± 0.02
	S-Mid AET	6.1 ± 0.0	7.8 ± 0.4	0.58 ± 0.01
	P-HnT AET	7.3 ± 0.3	11.1 ± 1.2	0.47 ± 0.00
	S-HnT AET	8.2 ± 0.6	14.2 ± 0.3	0.39 ± 0.02
	P-RD AET	4.9 ± 0.1	6.1 ± 0.1	0.65 ± 0.03
	S-RD AET	5.3 ± 0.4	6.8 ± 0.4	0.56 ± 0.01
Crosslinking Density	S-15% AET-1	4.9 ± 0.3	6.6 ± 0.4	0.32 ± 0.01
	S-15% AET-2	4.2 ± 0.3	6.0 ± 0.1	0.30 ± 0.01
	S-15% AET-3	4.1 ± 0.1	5.7 ± 0.1	0.31 ± 0.02
	S-15% AET-4	4.2 ± 0.3	5.9 ± 0.3	0.26 ± 0.02

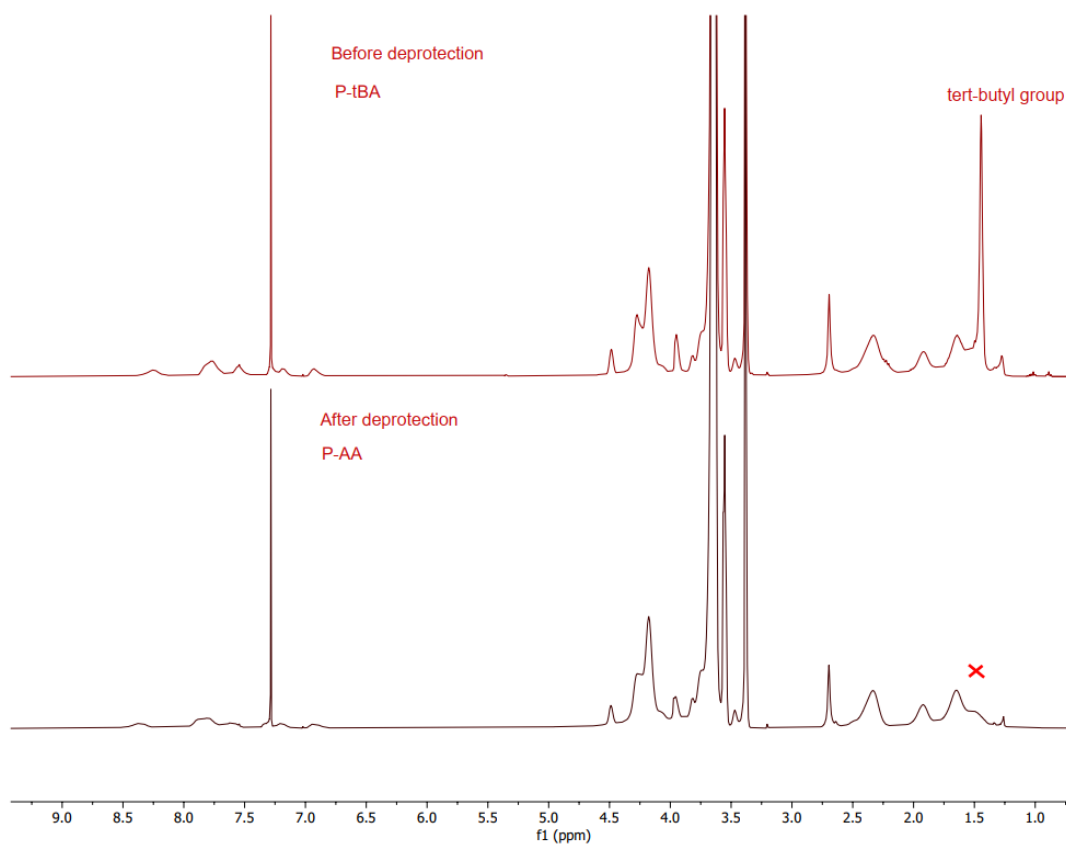


Figure S22. ¹H NMR spectra of the copolymer in CDCl₃ before (P-tBA, upper) and after (P-AA, lower) deprotection of tert-butyl groups.

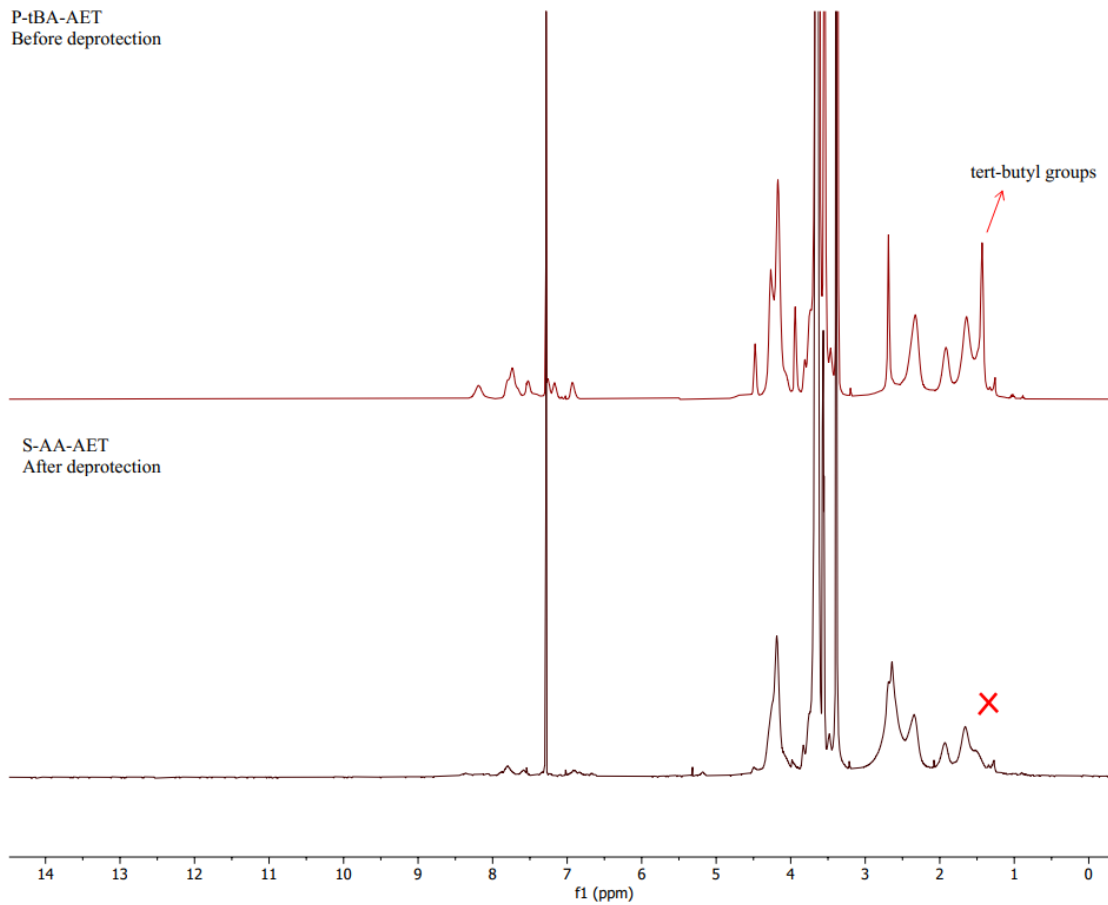


Figure S23. ¹H NMR spectra of copolymer in CDCl₃ before (P-tBA-AET, upper) and after (S-AA-AET, lower) deprotection of tert-butyl groups.

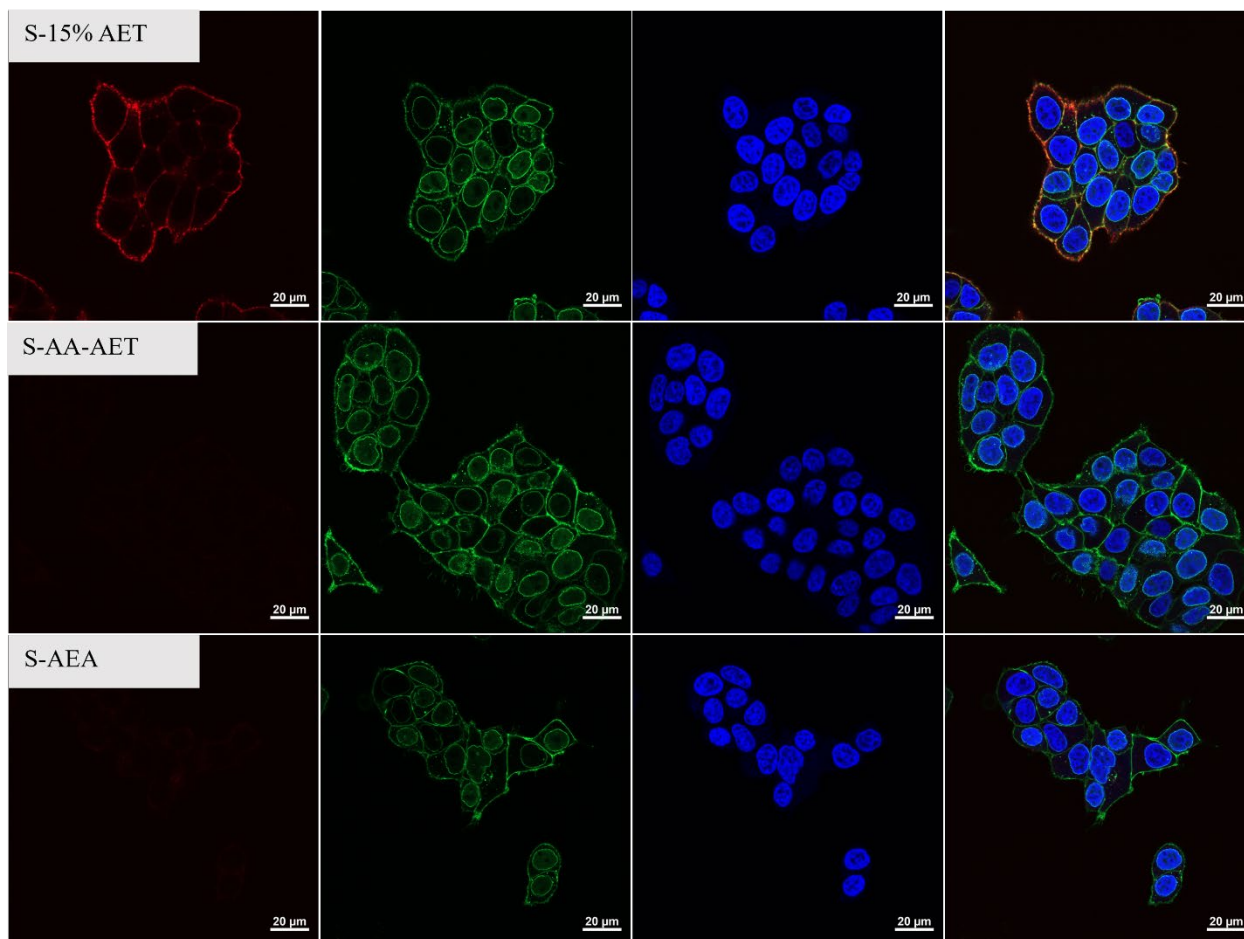


Figure S24. CLSM images of MCF-7 cells incubated with SCNPs with different charge types. Cells were incubated with Cy5-labeled NPs (red) at a concentration of $100 \mu\text{g mL}^{-1}$, 4°C for 2 hours. Nuclei and membrane were stained with Hoechst (blue) and wheat germ agglutinin (WGA) (green), respectively. This figure has the same setting as **Figure 2c**.

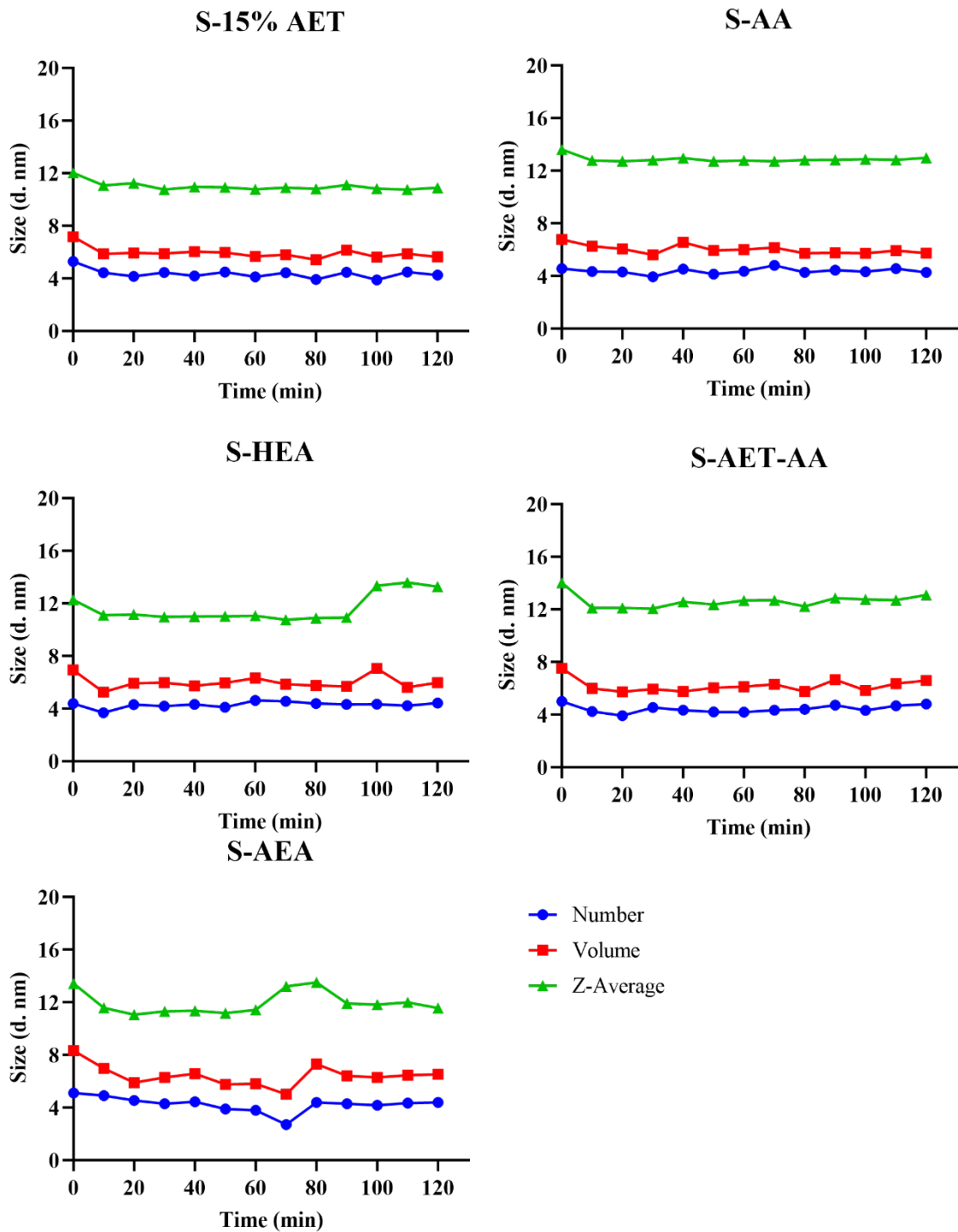


Figure S25. Stability study of SCNPs with different charge types at 37°C in complete DMEM cell medium. Data was collected from DLS over time, and the polymer concentration was 1 mg mL⁻¹.

Charge density

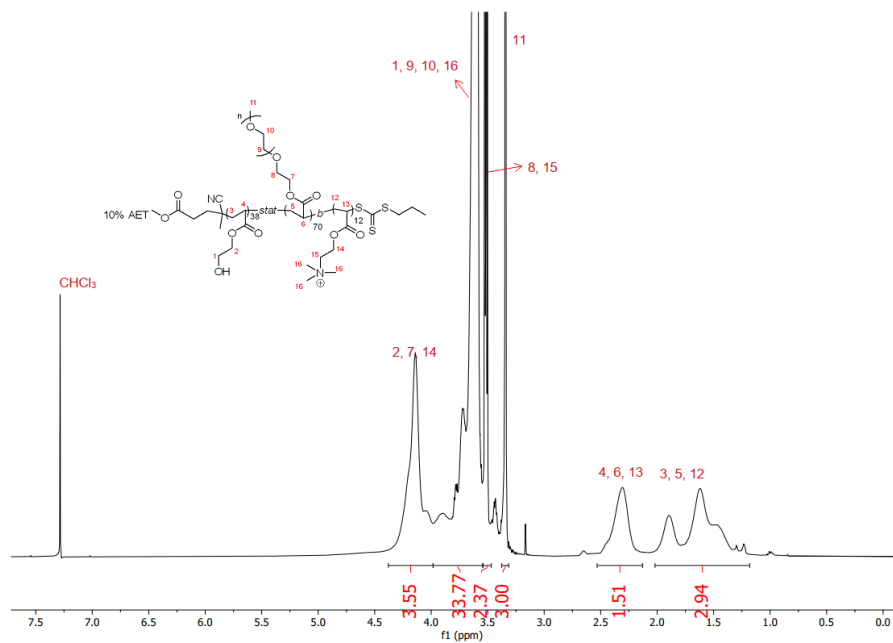


Figure S26. ¹H NMR spectrum of copolymer 10% AET in CDCl₃

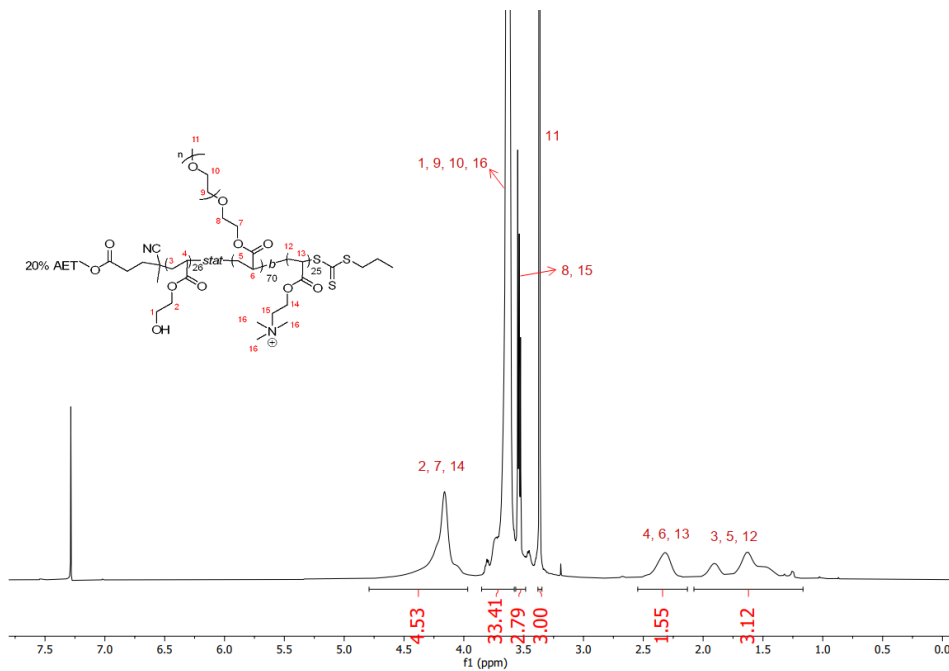


Figure S27. ¹H NMR spectrum of copolymer 20% AET in CDCl₃

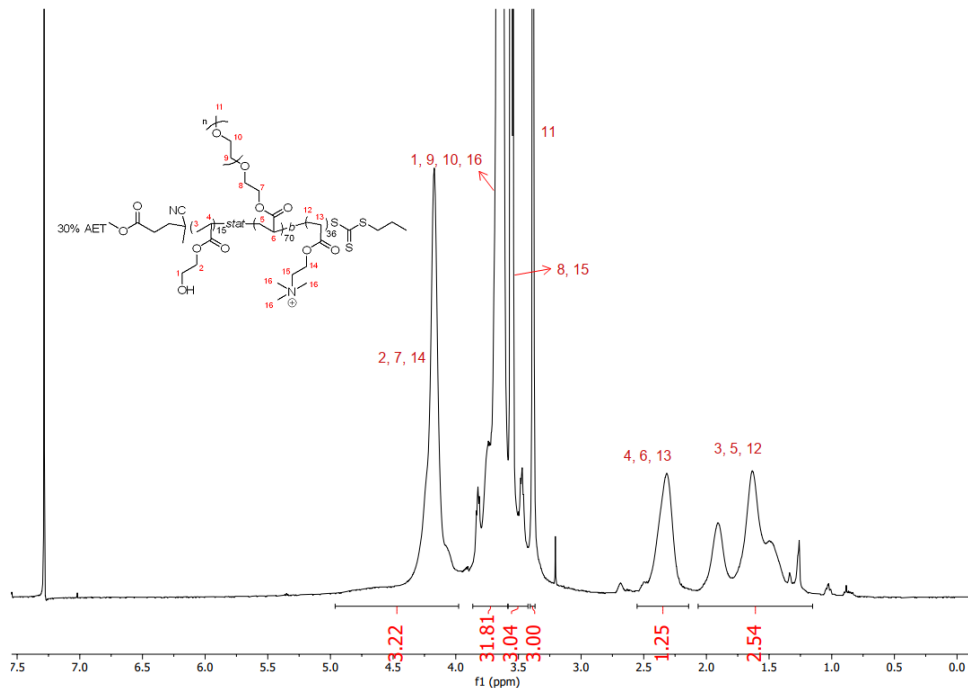


Figure S28. ^1H NMR spectrum of copolymer 30% AET in CDCl_3

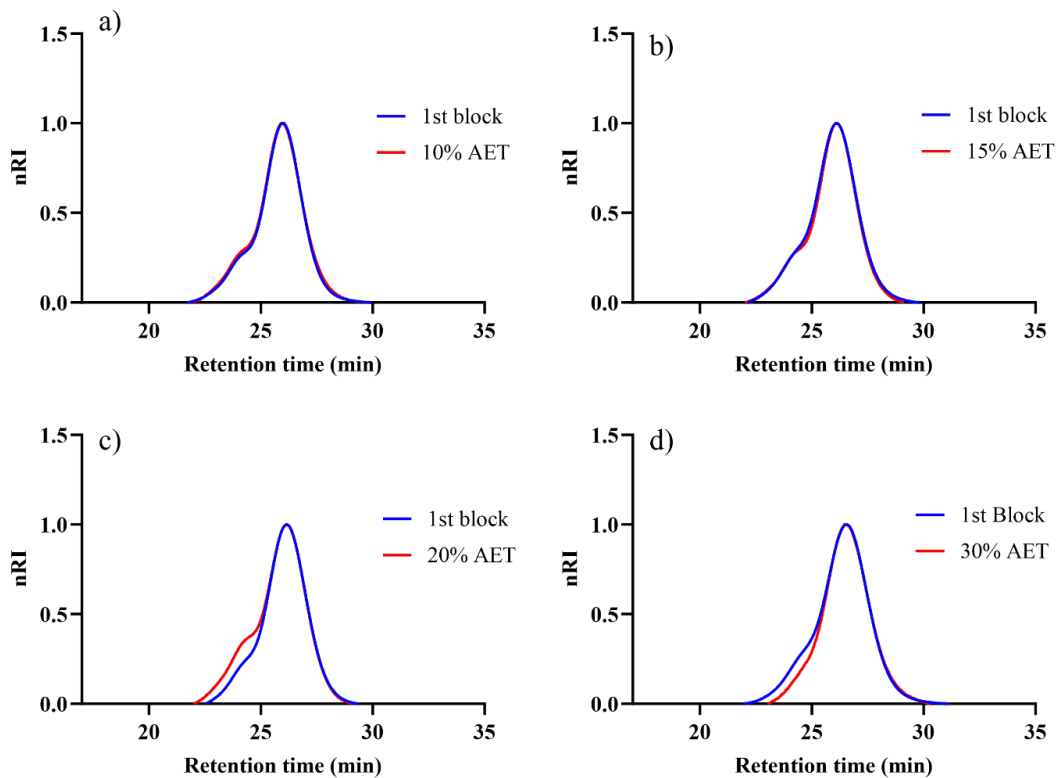


Figure S29. SEC traces in DMF of polymer backbones with different charge densities. Data was collected from RI detection, and DMF was used as the eluent.

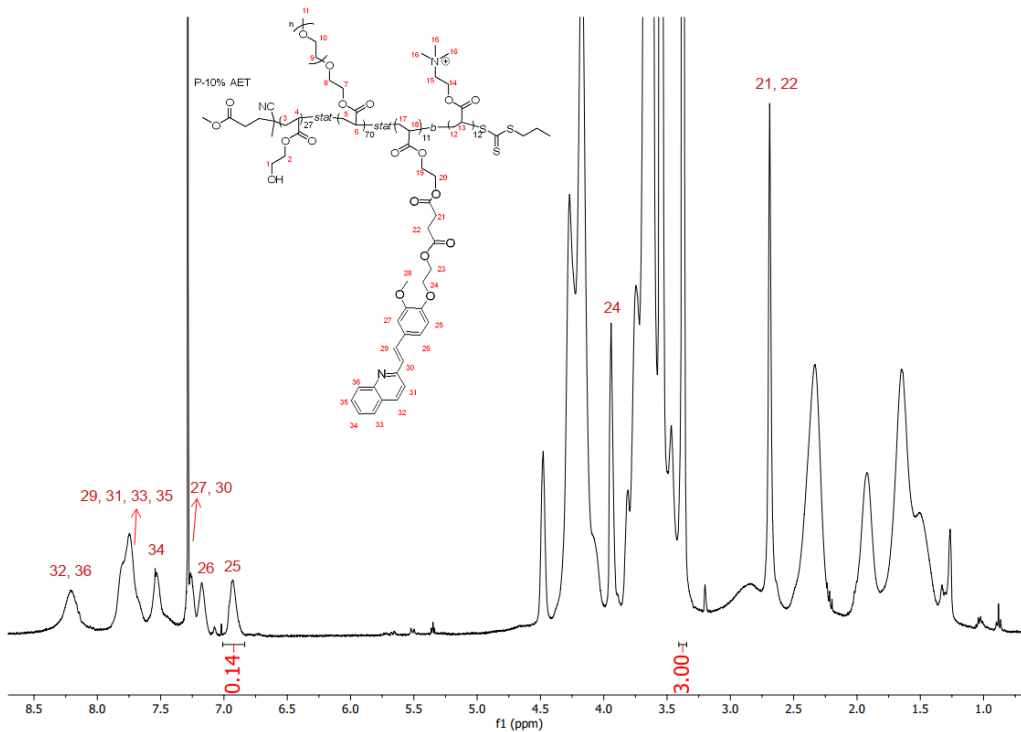


Figure S30. ¹H NMR spectrum of copolymer P-10% AET in CDCl₃.

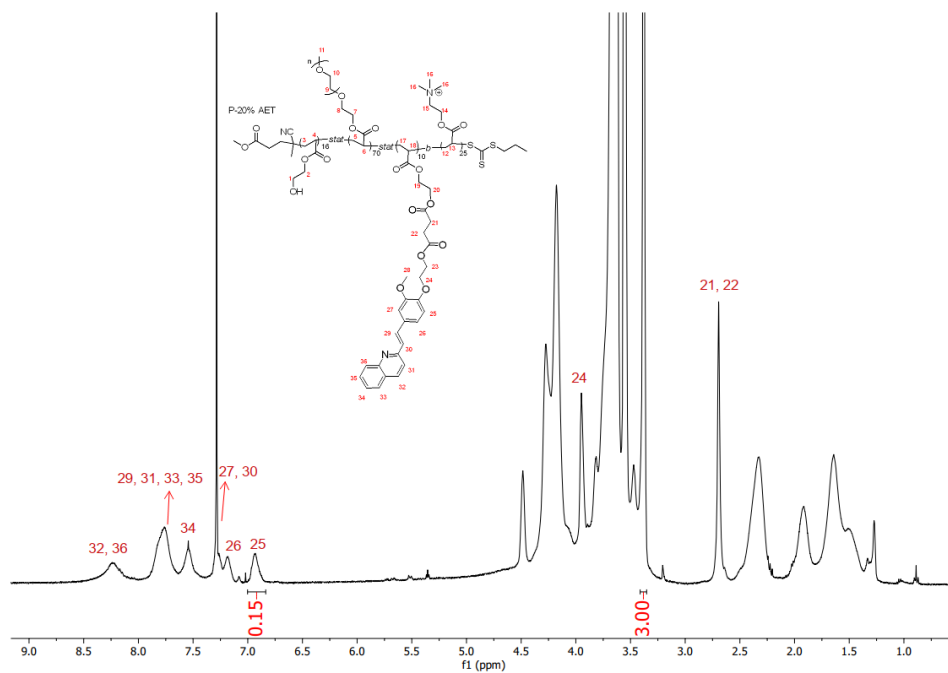


Figure S31. ¹H NMR spectrum of copolymer P-20% AET in CDCl₃.

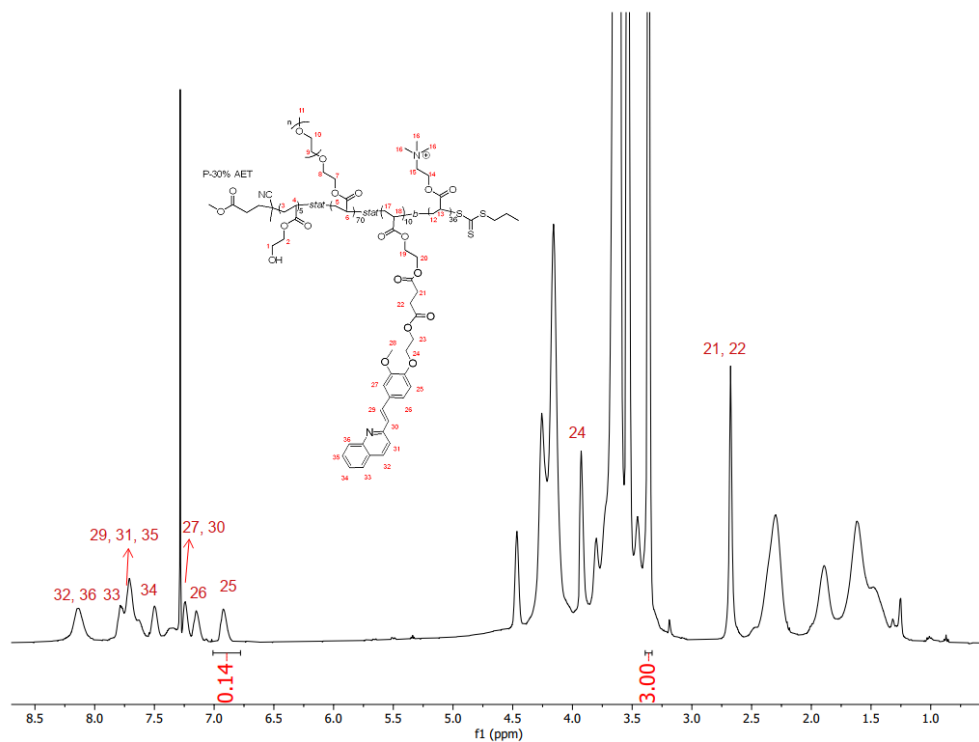


Figure S32. ^1H NMR spectrum of copolymer P-30% AET in CDCl_3 .

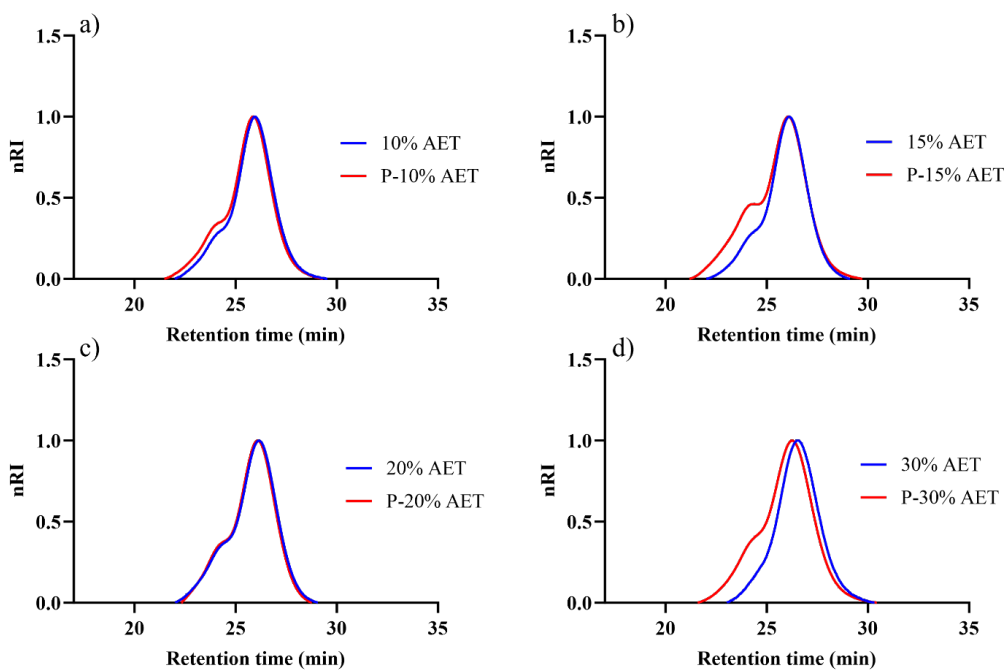


Figure S33. SEC traces of polymer with different charge densities before (blue) and after (red) crosslinker conjugation. Data was collected from RI detection, and DMF was used as the eluent.

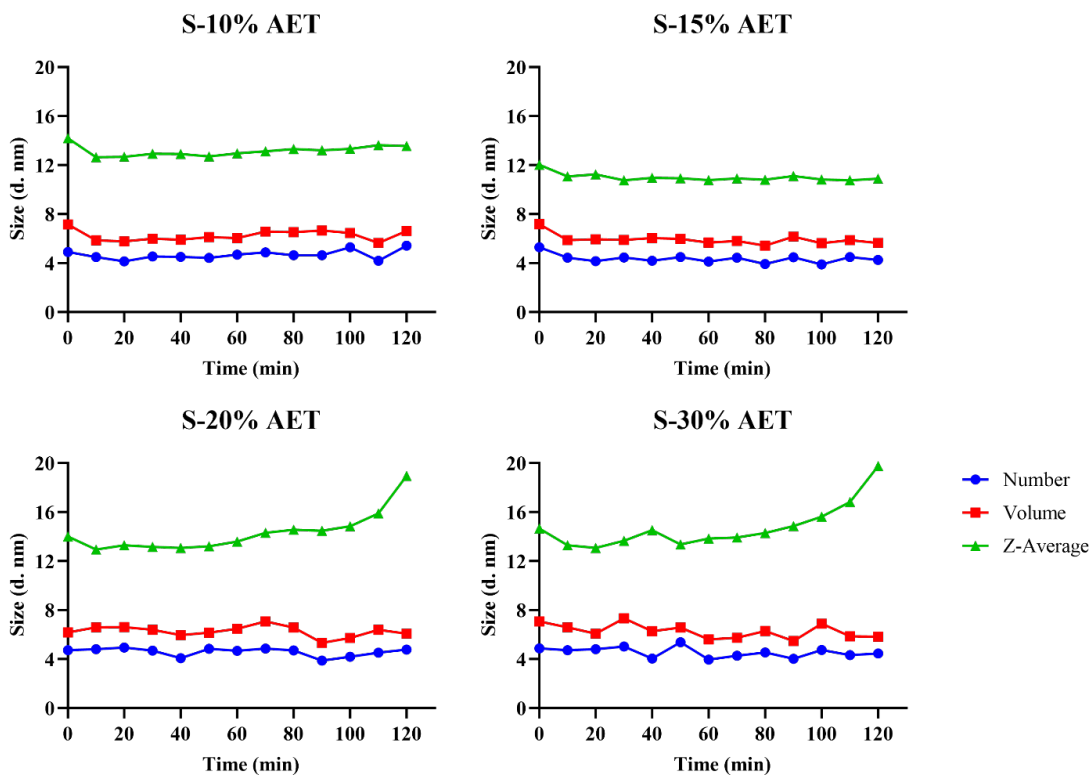


Figure S34. Stability study of SCNPs with different charge densities at 37°C in complete DMEM cell medium. Data was collected from DLS over time; polymer concentration is 1 mg mL⁻¹

Charge Position

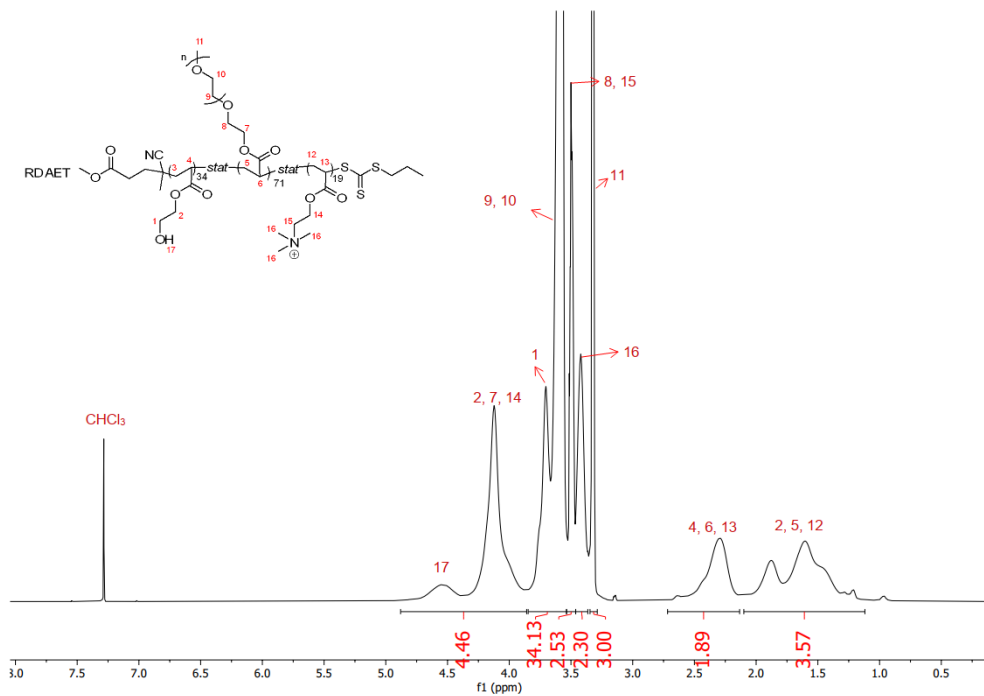


Figure S35. ^1H NMR spectrum of copolymer RDAET in CDCl_3

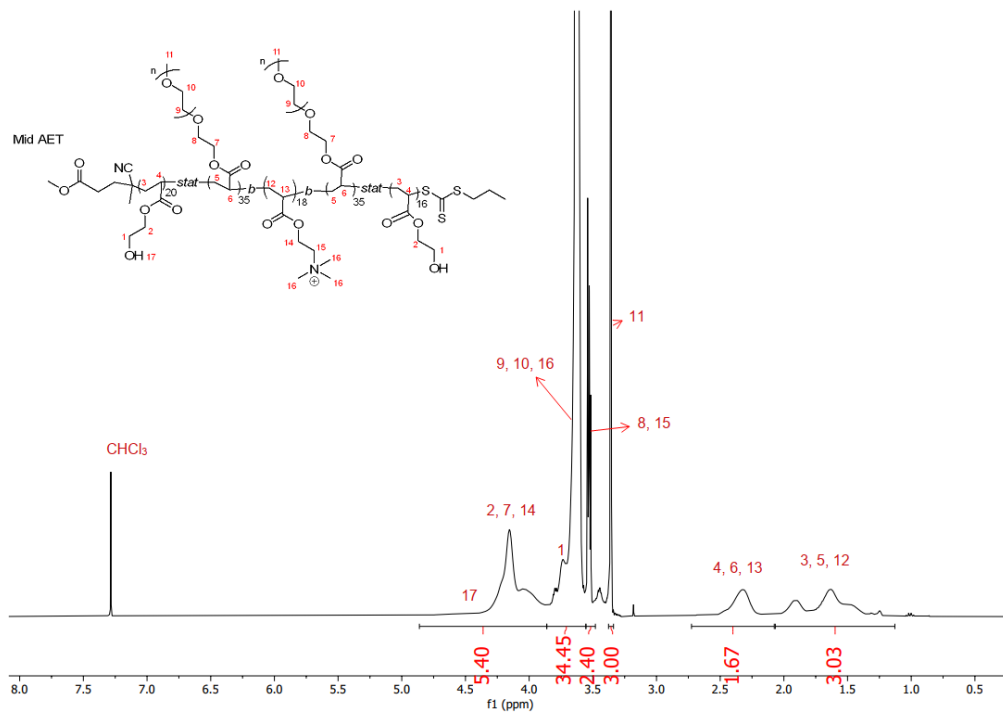


Figure S36. ^1H NMR spectrum of copolymer Mid AET in CDCl_3

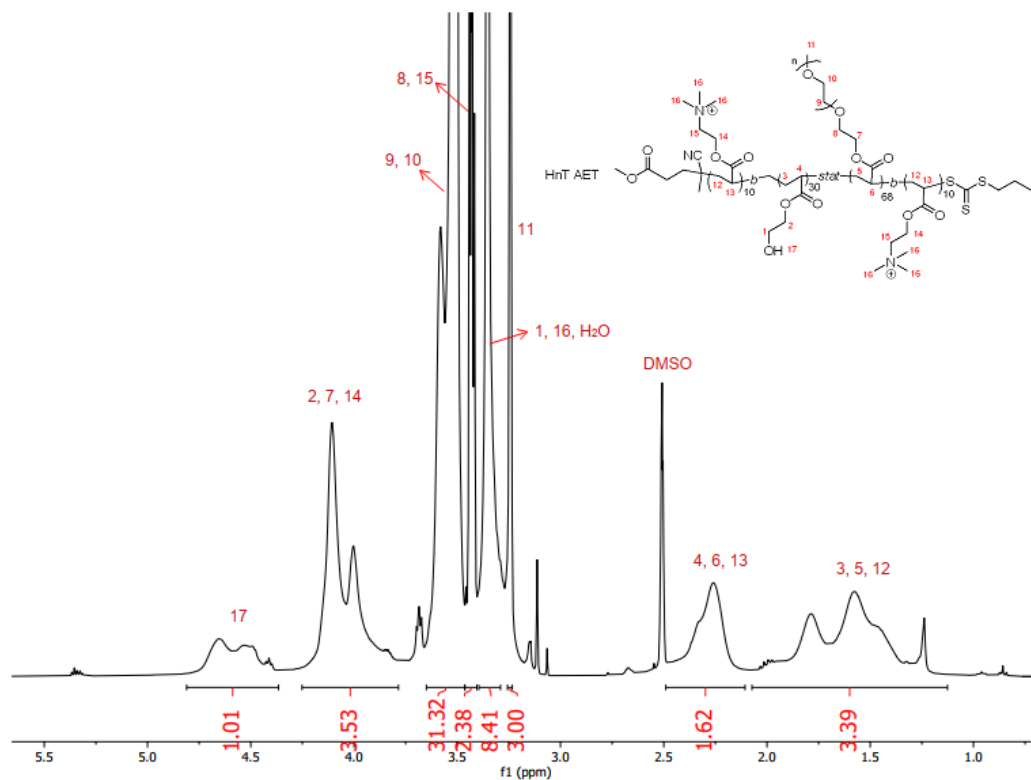


Figure S37. ^1H NMR spectrum of copolymer HnT AET in DMSO-d_6 .

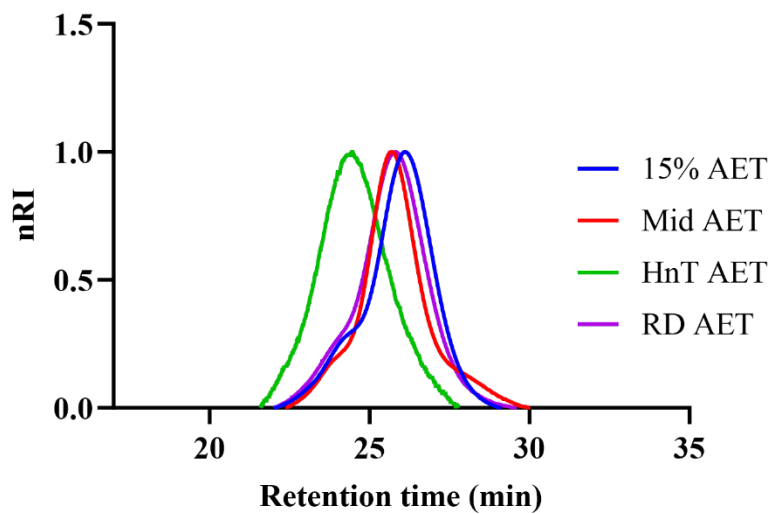


Figure S38. SEC traces of polymer backbones with different charge positions. Data was collected from RI detection, and DMF was used as the eluent.

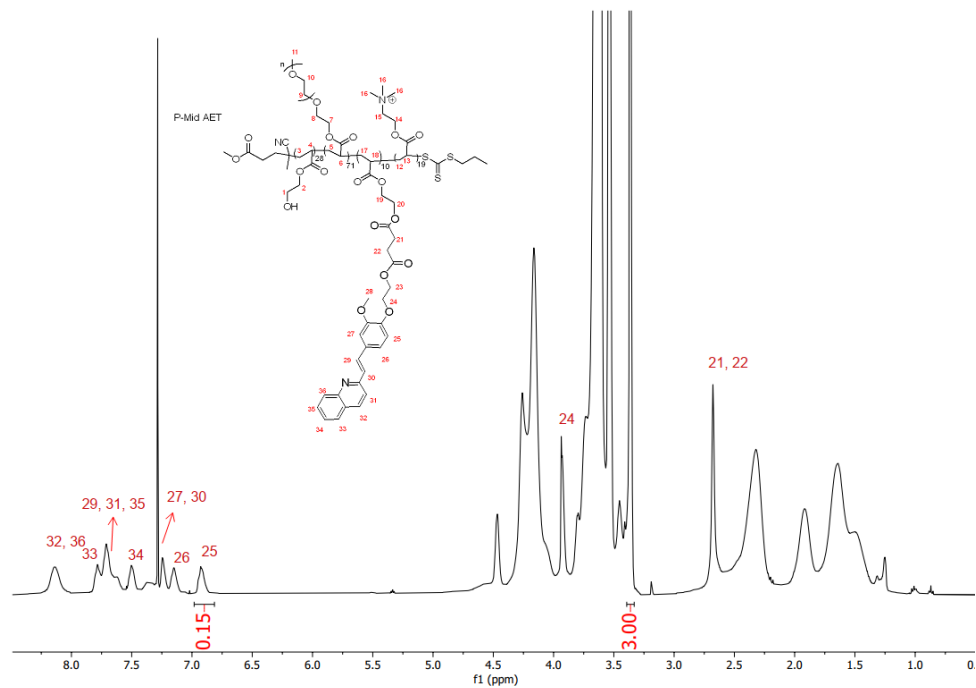


Figure S39. ¹H NMR spectrum of copolymer P-Mid AET in CDCl₃.

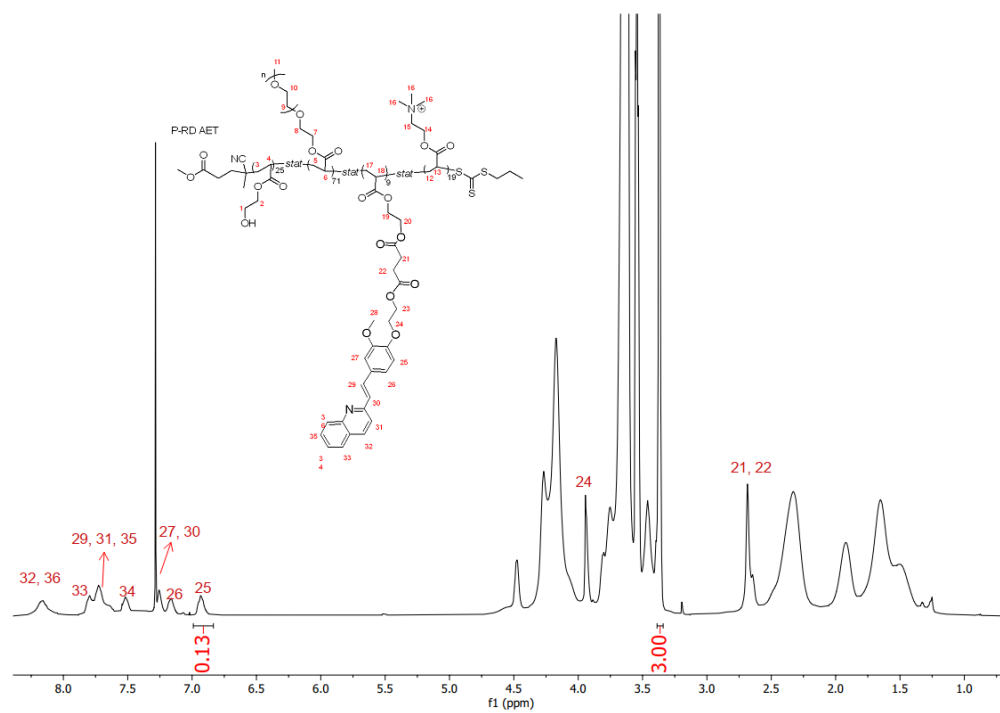


Figure S40. ¹H NMR spectrum of copolymer P-RD AET in CDCl₃.

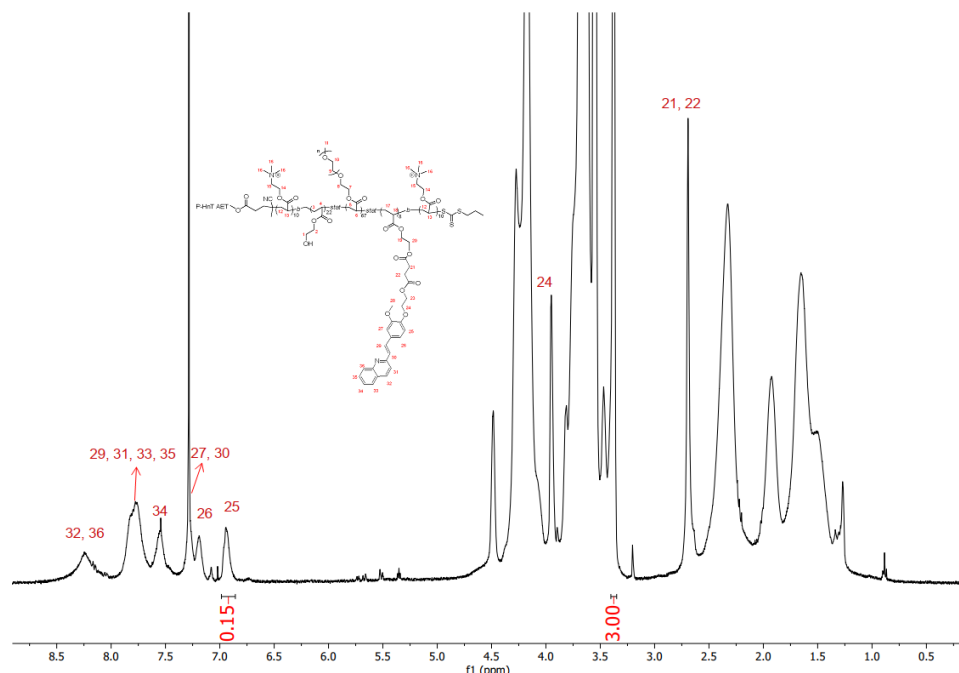


Figure S41. ^1H NMR spectrum of copolymer P-HnT AET in CDCl_3 .

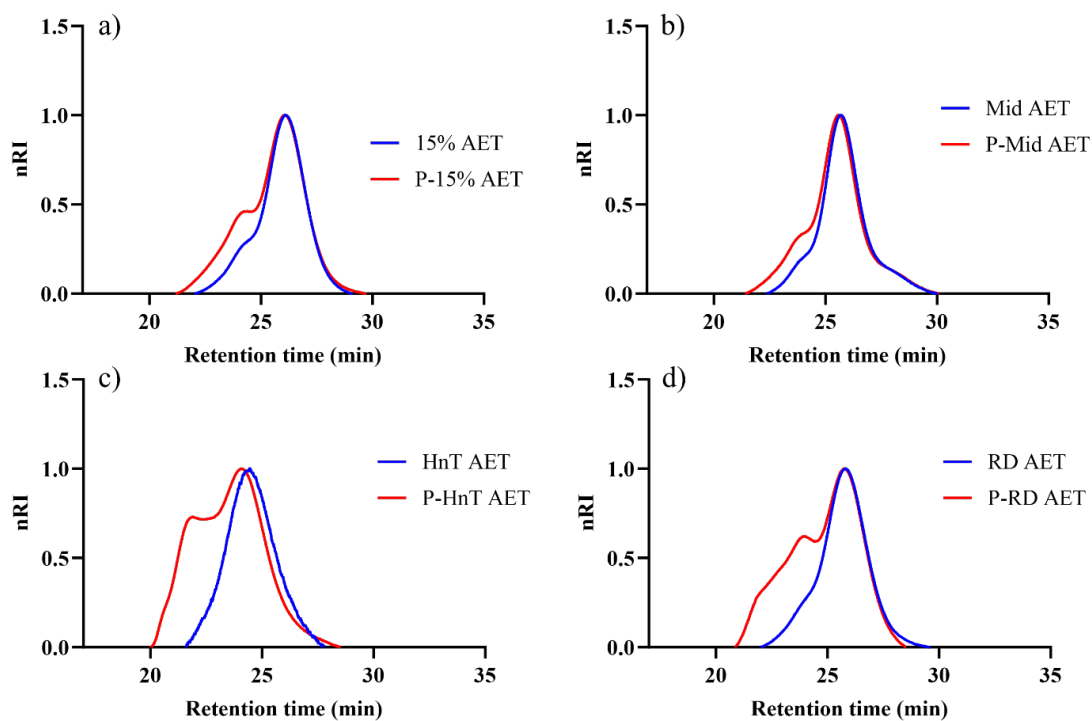


Figure S42. SEC traces of polymers with different charge positions before (blue) and after (red) the crosslinker conjugation. Data was collected from RI detection, and DMF was used as the eluent.

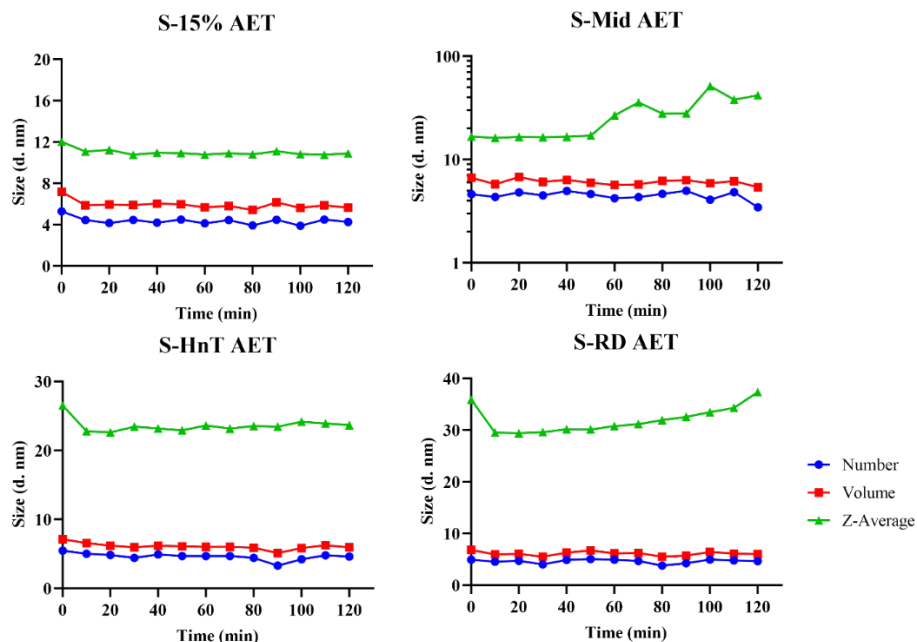


Figure S43. Stability study of SCNPs with different charge positions at 37°C in complete DMEM cell medium. Data was collected from DLS over time. Polymer concentration is 1 mg mL⁻¹

Crosslinking density

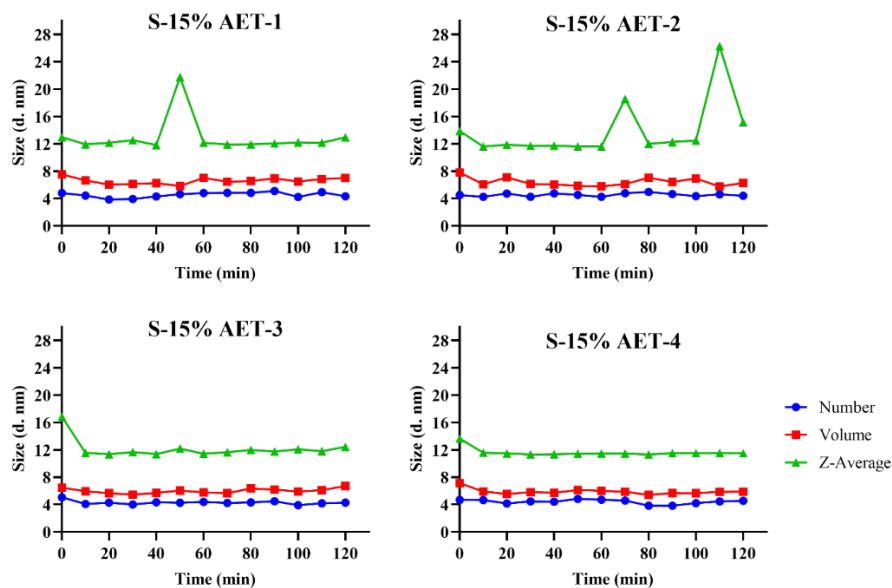


Figure S44. Stability study of SCNPs with different crosslinking densities at 37°C in complete DMEM cell medium. Data was collected from DLS over time, and the polymer concentration was 1 mg mL⁻¹.

References

1. N. M. Kirby, S. T. Mudie, A. M. Hawley, D. J. Cookson, H. D. T. Mertens, N. Cowieson and V. Samardzic-Boban, *J. Appl. Crystallogr.*, 2013, **46**, 1670-1680.
2. DANSE SasView for Small Angle Scattering Analysis, (<http://www.sasview.org>).
3. S. Kline, *J. Appl. Crystallogr.*, 2006, **39**, 895-900.
4. X. Xu, A. E. Smith, S. E. Kirkland and C. L. McCormick, *Macromolecules*, 2008, **41**, 8429-8435.